Fission Reaction Event Yield Algorithm

FREYA 2.0.2

User Manual

J. M. Verbeke[1], J. Randrup[2], R. Vogt[1,3]
[1]Lawrence Livermore National Laboratory, P.O. Box 808, Livermore, CA 94551, USA
[2]Lawrence Berkeley National Laboratory, 1 Cyclotron Road, Berkeley, CA 94720, USA
[3]University of California, Davis, One Shields Avenue, Davis, CA 95616, USA

Abstract

From nuclear materials accountability to detection of special nuclear material, SNM, the need for better modeling of fission has grown over the past decades. Current radiation transport codes compute average quantities with great accuracy and performance, but performance and averaging come at the price of limited interaction-by-interaction modeling. For fission applications, these codes often lack the capability of modeling interactions exactly: energy is not conserved, energies of emitted particles are uncorrelated, prompt fission neutron and photon multiplicities are uncorrelated. Many modern applications require more exclusive quantities than averages, such as the fluctuations in certain observables (e.g. the neutron multiplicity) and correlations between neutrons and photons. The new computational model, FREYA 2.0.2 (Fission Reaction Event Yield Algorithm), aims to meet this need by modeling complete fission events. Thus it automatically includes fluctuations as well as correlations resulting from conservation of energy and momentum. FREYA 2.0.2 has been integrated into the LLNL Fission Library 2.0.2, and will soon be part of MCNP6.2, TRIPOLI-4.10, and Geant4.10.

Copyright notices

Copyright notice specific to the LLNL Fission Library

Copyright notice specific to FREYA

1 Introduction

Several general-purpose Monte Carlo codes (MCNP/X [1–5], TART [5,6], COG [5,7], Geant [8], etc.) are currently available for modeling neutron transport. To model fission, they employ the "average fission model", which is characterized by outgoing projectiles (fission neutrons and photons) that are uncorrelated and sampled from the same probability density function. This approximation is sufficient for the calculation of average quantities such as flux, energy deposition and multiplication. However, it is unsuitable for studying detailed correlations between neutrons and/or photons on an event-by-event basis.

During the past decade several code extensions have been developed that allow the modeling of correlations in fission. MCNP-DSP [5, 9] and MCNPX-PoliMi [5, 10] added angular correlations of fission neutrons by assuming the ^{252}Cf spontaneous fission distribution can be employed for all fissionable nuclides. Both codes also include detailed multiplicity and energy distributions for prompt fission photons time correlated with the fission event. A new option was introduced in MCNPX2.7.0 [11] for the treatment of fission events utilizing a library developed at LLNL [12]. It features time-correlated sampling of photons from neutron-induced fission, photofission and spontaneous fission. The capabilities for correlations are, however, limited for these last 3 options (MCNP-DSP, MCNPX-PoliMi, LLNL Fission Library), as they sample outgoing particles from average fission distributions instead of sampling them from individual realizations of a fission process.

In recent years, various simulation treatments have made it possible to also address fluctuations of and correlations between fission observables. In particular, a Monte Carlo approach was developed [13, 14] for the sequential emission of neutrons and photons from individual fission fragments in binary fission. The more recent event-by-event fission model, FREYA, includes more fission isotopes and has been specifically designed for producing large numbers of fission events in a fast simulation [15–20]. Employing nuclear data for fragment-mass and kinetic-energy distributions, using statistical evaporation models for neutron and photon emission, and conserving energy, momentum, and angular momentum throughout, FREYA is able to predict a host of correlation observables, including correlations in neutron multiplicity, energy, and angles, and the energy sharing between neutrons and photons.

The stand-alone fission event generator FREYA was integrated into the LLNL Fission Library, which is an integral part of the transport codes MCNPX2.7.0, MCNP6, TRIPOLI-4.9 [21], and Geant4.10.

The first part of this paper will focus on the physics in the FREYA fission model and the algorithmic implementation thereof, the second part will describe the data files required by FREYA, while the third part will show how to use FREYA within the LLNL Fission Library.

Readers only interested in the differences between FREYA versions 1.0 and 2.0.2 are encouraged to read Ref. [22], which summarizes those differences.

2 Fission model and algorithm

The computational model FREYA generates complete fission events, *i.e.* it provides the the full kinematic information on the two product nuclei as well as all the emitted neutrons and photons. In its development, an emphasis had been put on speed, so large event samples can be generated fast, and FREYA therefore relies on experimental data supplemented by physics-based modeling.

The algorithmic flow of FREYA is illustrated in Figs. 1-8. Blue boxes indicate entry points, parallelograms input parameters, cylinders data files, diamonds decision points, pentagons off page connectors, orange ovals outputs, and dice indicate sampling.

FREYA models the fission of excited nuclei. Finite excitation energies can be generated in a variety of ways, including electromagnetic agitation and, more commonly for current applications, absorption of a neutron by a fissile nucleus. In this case, the fissile nucleus $^{A_0}Z_0$ is in its ground state $E_0^* = 0$ before the incident neutron

is absorbed, see blue box in Fig. 1; Z_0, A_0, and E_n are entered where E_n is the kinetic energy of the incoming neutron absorbed by the specified fissile nucleus ${}^{A_0}Z_0$. In its simplest version, FREYA assumes that the initial nucleus ${}^{A_0}Z_0$ is at rest, therefore $P_0 = 0$.

Depending on its degree of excitation, the system may emit one or more neutrons prior to fission, either by pre-equilibrium emission (at the highest excitations) or by (possibly sequential) pre-fission evaporation which may continue as long as the excitation energy exceeds the neutron separation energy. The two processes are described in Figs. 1-2.

In the case of spontaneous fission, the fissile nucleus ${}^{A_0}Z_0$ fissions with no prior neutron absorption, and the excitation energy of the nucleus is $E_0^* = 0$, see blue box in Fig. 3.

After the system is prepared for either neutron-induced or spontaneous fission, the fission fragments are selected by sampling, as described in Fig. 3. The scission process is finalized by determining the fission Q value, as in Fig. 4. The fission fragment kinetic and excitation energies are then determined, as shown in Figs. 5-6. Finally, neutron evaporation and photon emission from the fragments, as shown in Figs. 7-8, complete the fission event.

This section is divided into three parts to describe the physics behind the algorithms in FREYA. The system pre-fission is described in Sec. 2.1. Next, the scission process itself that results in binary fission with two excited fission fragments is treated in Sec. 2.2. Finally, de-excitation by post-fission radiation of neutrons and photons is described in Sec. 2.3.

2.1 Pre-fission radiation

In addition to spontaneous fission, FREYA treats neutron-induced fission up to $E_n = 20\,\mathrm{MeV}$. There are two possible ways for neutrons to be emitted before fission occurs for sufficiently high incident neutron energies: pre-equilibrium neutron emission (which plays a role at the highest energies) and pre-fission neutron evaporation, referred to as multichance fission. FREYA handles both these possibilities.

2.1.1 Pre-equilibrium neutron emission

Pre-equilibrium neutron emission occurs if a neutron is emitted before the compound nucleus is equilibrated. In this case, a non-equilibrium model employing a two-component exciton model that represents the evolution of the nuclear reaction in terms of time-dependent populations of ever more complex many-particle-many-hole states is used. See Ref. [18] for more details.

A many-exciton state consists of $p_{\nu(\pi)}$ neutron (proton) particle excitons and $h_{\nu(\pi)}$ neutron (proton) hole excitons. The total number of neutron (proton) excitons in the state is $n_{\nu(\pi)} = p_{\nu(\pi)} + h_{\nu(\pi)}$. Processes that reduce the number of excitons are neglected. The pre-equilibrium neutron emission spectrum is then given by

$$\frac{d\sigma_n}{dE} = \sigma_{\mathrm{CN}} \sum_{p_\pi=0}^{p_\pi^{\max}} \sum_{p_\nu=1}^{p_\nu^{\max}} W(p_\pi,h_\pi,p_\nu,h_\nu,E)\,\tau(p_\pi,h_\pi,p_\nu,h_\nu)\,P(p_\pi,h_\pi,p_\nu,h_\nu) \tag{1}$$

where σ_{CN} is the compound nuclear cross section (usually obtained from an optical model calculation), W is the rate for emitting a neutron with energy E from the exciton state $(p_\pi,h_\pi,p_\nu,h_\nu)$, τ is the lifetime of this state, and $P(p_\pi,h_\pi,p_\nu,h_\nu)$ is the (time-averaged) probability for the system to survive the previous stages and arrive at the specified exciton state. In the two-component model, contributions to the survival probability from both particle creation and charge exchange need to be accounted for. The survival probability for the exciton state $(p_\pi,h_\pi,p_\nu,h_\nu)$ can be obtained from a recursion relation starting from the initial condition $P(p_\nu=1,h_\nu=0,p_\pi=0,h_\pi=0) = 1$ and setting $P=0$ for terms with negative exciton number.

For each event generated, FREYA first considers the possibility of pre-equilibrium neutron emission and, if it occurs, a neutron is emitted with an energy selected from the calculated pre-equilibrium spectrum, Eq. (1). The

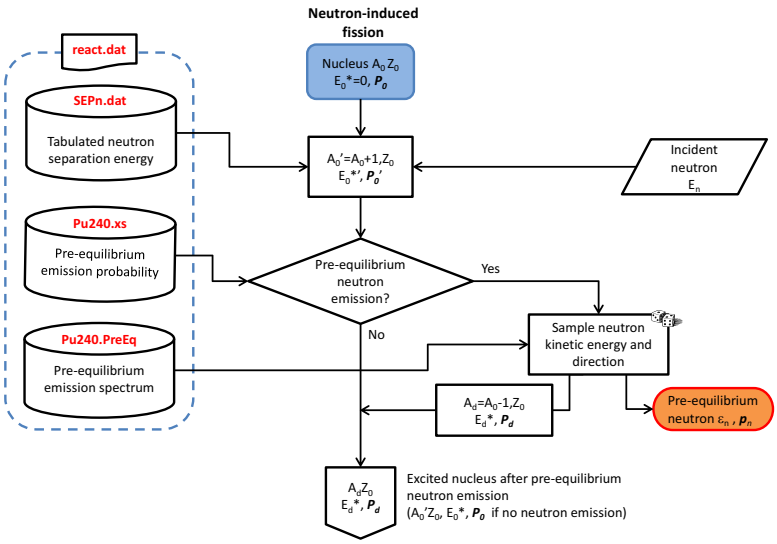

Figure 1: Pre-equilibrium neutron emission, associated with neutron-induced fission, for the example of ^{239}Pu(n,f).

possibility of equilibrium neutron evaporation is then considered, starting either from the original compound nucleus, e.g. ^{240}Pu* for ^{239}Pu(n,f), or the less excited nucleus, ^{239}Pu*, remaining after pre-equilibrium emission has occurred. Neutron evaporation continues until the excitation energy of a daughter nucleus is below the fission barrier (in which case the event is abandoned and a new event is generated) or the nucleus fissions.

A flow chart for pre-equilibrium neutron emission is shown in Fig. 1. One should note that pre-equilibrium neutron emission is very mprobable, on average 0.10 pre-equilibrium neutrons are emitted at $E_n \sim 14$ MeV, see Fig. 2 in Ref. [18]. After this first process, the excited nucleus can also undergo pre-fission neutron evaporation, discussed next.

2.1.2 Pre-fission neutron evaporation

In multichance fission or pre-fission neutron evaporation — shown in Fig. 2 — neutron evaporation can occur from the compound nucleus as long as the excitation energy of the compound exceeds the neutron separation energy, S_n. One or more neutrons can be emitted before fission. The probability for pre-fission neutron evaporation is determined by the competition between fission and neutron evaporation. At higher incident neutron energies, neutron evaporation from the compound nucleus competes more favorably with direct (first chance) fission.

The criterion for pre-fission evaporation is based on $\Gamma_n(E^*)/\Gamma_{\rm f}(E^*)$, the relative magnitudes of the neutron evaporation and fission decay widths at a given excitation energy E^* [23],

$$\frac{\Gamma_n(E^*)}{\Gamma_{\rm f}(E^*)} = \frac{2g_{\rm n}\mu_n\sigma}{\pi\hbar^2}\frac{\int_0^{X_n}(X_n-x)\rho_n(x)dx}{\int_0^{X_{\rm f}}\rho_{\rm f}(x)dx}\,, \tag{2}$$

where $g_s = 2$ is the spin degeneracy of the neutron, μ_n is its reduced mass, and $\sigma = \pi R^2 = \pi r_0^2 A^{2/3}$. Here $\rho_n(x)$ is the level density in the evaporation daughter nucleus at excitation energy x. The maximum value of x is given $X_n = Q_n = E^* - S_n$, where Q_n is the Q value for neutron emission and S_n is the neutron separation energy. Similarly, $\rho_{\rm f}(x)$ is the level density of the fissioning nucleus when its shape is that associated with the top of the fission barrier. The excitation x is measured relative to the barrier top with a maximum value of $X_{\rm f} = E^* - B_{\rm f}$, where $B_{\rm f}$ is the height of the fission barrier.

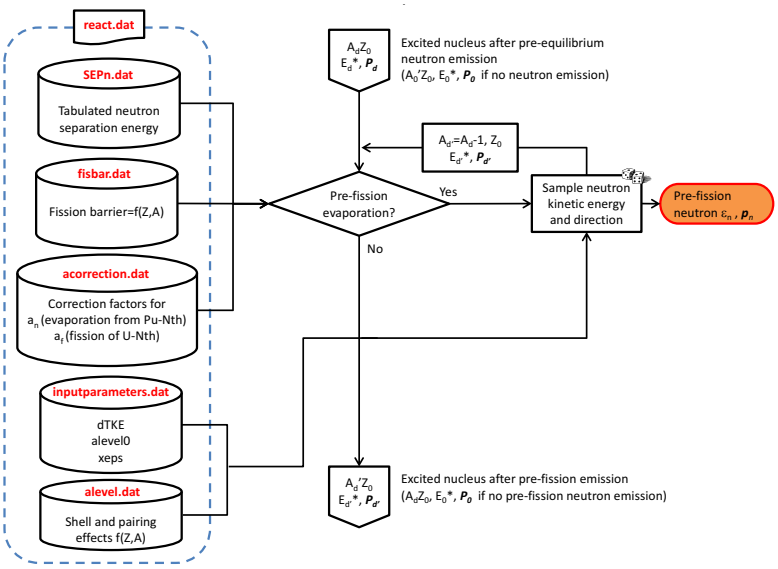

Figure 2: Pre-fission evaporation, associated with neutron-induced fission.

Neutron evaporation is possible whenever the excitation energy of the compound nucleus is larger than the neutron separation energy, $E^* > S_n$, a positive quantity because it costs energy to remove a neutron from the nucleus. The excitation energy of the evaporation daughter nucleus is $E_d^* = E^* - S_n - E$ where E is the kinetic energy of the relative motion between the emitted neutron and the daughter nucleus. If this quantity exceeds the fission barrier in the daughter nucleus, then second-chance fission is possible. The same procedure is then applied to the daughter nucleus, so that further pre-fission neutron emission possible. As the incident neutron energy is increased, emission of further pre-fission neutrons becomes possible and the associated fission events may be classified as first-chance fission (when there are no pre-fission neutrons emitted), second-chance fission (when one neutron is emitted prior to fission), and so on. See Fig. 1 of Ref. [18] for a plot of the multichance fission probability up to $E_n = 20$ MeV for ^{239}Pu(n,f).

Emitted neutron kinetic energies are sampled using an algorithm similar to neutron evaporation explained in Sec. 2.3.1. For more discussion, see Ref. [18].

After both pre-equilibrium neutron emission and pre-fission neutron evaporation, the excitation energy is adjusted and the energy at which the yields are sampled is reduced accordingly.

2.2 Fission

After pre-fission radiation, the mass and charge of the initial compound nucleus is partitioned among the two fission fragments and the available energy is divided between the excitation of the two fragments and their relative kinetic energy.

2.2.1 Fission fragment mass and charge distributions

The current understanding of the fission process is that the evolution from the initial compound nucleus to two distinct fission fragments occurs gradualy as a result of a dissipative multidimensional evolution of the nuclear shape. Because no quantitatively reliable theory has yet been developed for this process, we employ empirical evidence as a basis for selecting the mass and charge parition.

To treat a given fission case, we need the fission fragment mass distribution $Y(A_f)$ and the total kinetic energy TKE(A) for the particular excitation energy considered. $Y(A_f)$ is taken either directly as the measured yields or as a five-gaussian fit to the data which makes it possible to parametrize its energy dependence.

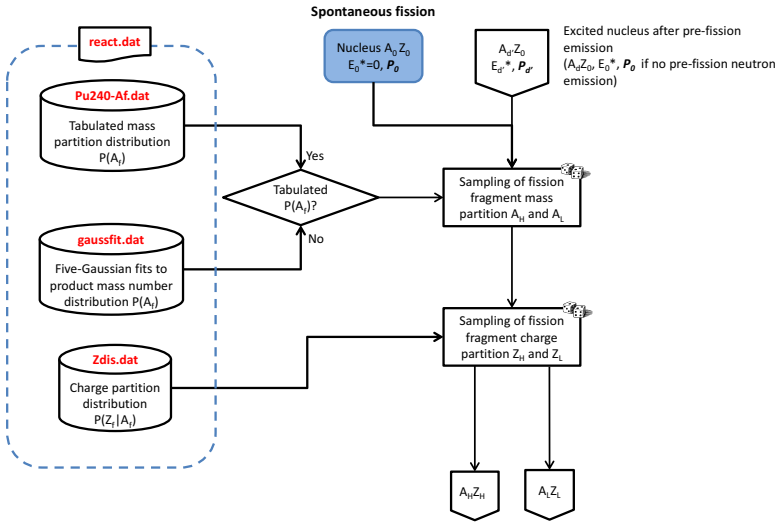

Figure 3: Selection of fission fragments, applicable both to neutron-induced and spontaneous fission, for the example of ^{239}Pu(n,f).

The compound nucleus left after pre-fission radiation undergoes binary fission into a heavy $^{A_H}Z_H$ and a light fragment $^{A_L}Z_L$, see Fig. 3. The mass split based on $Y(A_f)$ is first selected. The fragment masses are obtained from experimental mass yields $Y(A_f)$ — see Refs. [15, 17] — in the case of spontaneous fission. For neutron-induced fission, the energy dependence of $Y(A_f)$ has been modeled for incident neutron energies of up to 20 MeV [18]. When data are not available for the mass yields $Y(A_f)$, the mass number A_f of one of the fission fragments is selected randomly from a probability density $Y(A_f)$ for which we employ five-Gaussian fits to the product mass number distribution [24] shifted upward in mass to ensure a symmetric distribution of the primary fragments. Sec. 3.7 covers the five-Gaussian fits in more detail.

The charge partition is selected subsequently from the associated conditional probability distribution $P(Z_f|A_f)$. For this, we follow Ref. [25] and employ a Gaussian form

$$P(Z_f|A_f) \propto \exp\left(-\frac{(Z_f - \overline{Z}_f(A_f))^2}{2\sigma_Z^2}\right) \tag{3}$$

suggested by experiment [18] with the condition $\left|Z_f - \overline{Z}_f(A_f)\right| \leq 5\sigma_Z$. The centroid is determined by requiring that the fragments have, on average, the same charge-to-mass ratio as the fissioning nucleus $\overline{Z}_f(A_f) = A_f(Z_0/A_0)$. The charge of the complementary fragment then follows using $Z_L + Z_H = Z_0$.

2.2.2 Fragment energies

Once the mass and charge of the two fragments have been selected, the linear and angular momenta of the two fragments and their internal excitations are sampled. The Q-value of the fission channel is the difference between the total mass of A_0 and the fragment ground-state masses,

$$Q_{LH} = M(A_0)c^2 - M_L c^2 - M_H c^2 \,. \tag{4}$$

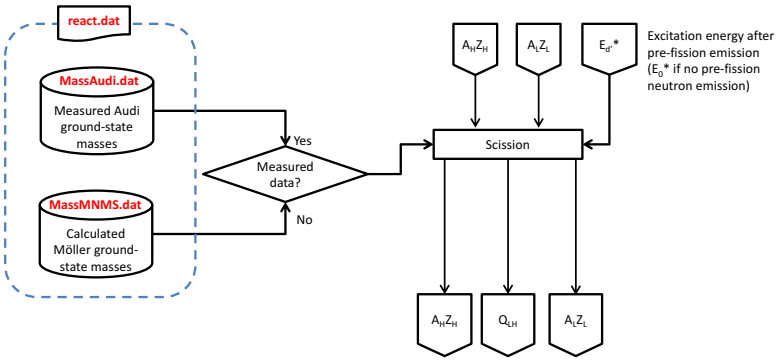

Figure 4: Scission, applicable both to neutron-induced and spontaneous fission.

FREYA takes the required nuclear ground-state masses from the compilation by Audi and Wapstra [26], supplemented by the calculated masses of Möller *et al.* [27] when no data are available. This simple process is shown in Fig. 4.

Figures 5-6 shows how the fission fragment energies are selected. The Q_{LH} value is divided between the total kinetic energy (TKE), the total rotational and statistical excitations of the fragments. The average TKE is assumed to take the form

$$\overline{\mathrm{TKE}}(A_H, E_n) = \overline{\mathrm{TKE}}_{\mathrm{data}}(A_H) + d\mathrm{TKE}(E_n) \,. \tag{5}$$

The first term is extracted from data on thermal neutrons while the second is adjusted to the measured average neutron multiplicity, $\overline{\nu}$.

After the average total fragment kinetic energy, $\overline{\mathrm{TKE}}$, has been calculated, the energy available for rotational and statistical excitation of the two fragments is then

$$E^*_{\mathrm{sc}} = Q - \overline{\mathrm{TKE}} \tag{6}$$

and the corresponding 'scission temperature' T_{sc} is obtained from

$$E^*_{\mathrm{sc}} = (A_0/e_0)T^2_{\mathrm{sc}} \,. \tag{7}$$

The inclusion of angular momentum in FREYA was described in Ref. [20]. The overall rigid rotation of the dinuclear configuration prior to scission, caused by the absorption of the incoming neutron and the recoil(s) from any evaporated neutron(s), dictates certain mean angular momenta in the two fragments. In addition,

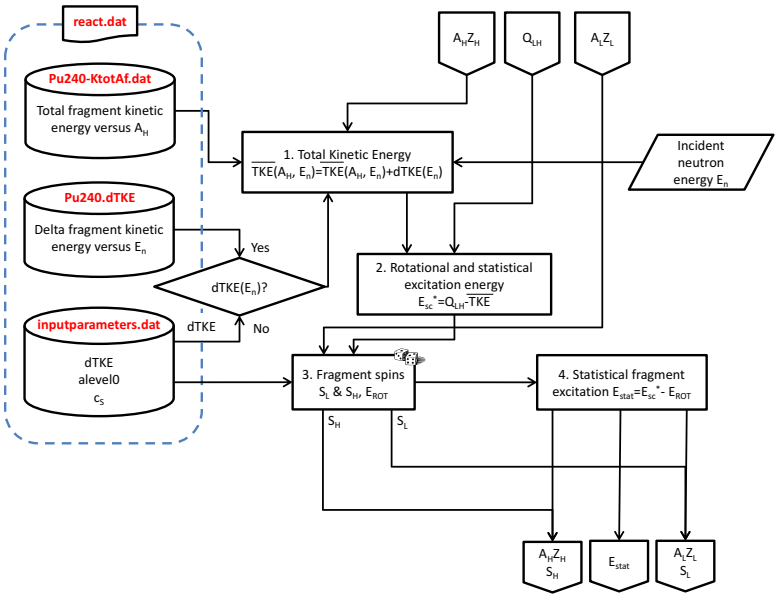

Figure 5: Selection of fission fragment rotational energies, new to FREYA 2.0.2, for the example of ^{239}Pu(n,f).

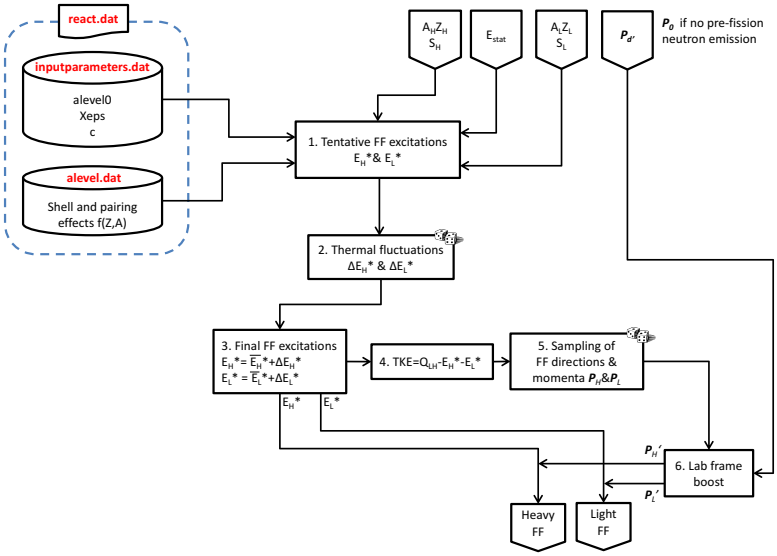

Figure 6: Selection of fission fragment excitations and momenta.

due to the statistical excitation of the scission complex, the fragments also acquire fluctuations around those mean values. FREYA includes fluctuations in the wriggling and bending modes (consisting of rotations in the same or opposite sense around an axis perpendicular to the dinuclear axis) but ignores tilting and twisting (in which the fragments rotate around the dinuclear axis). These dinuclear rotational modes are assumed to become statistically excited during scission and they are therefore described by Boltzmann distributions,

$$P_{\pm}(s_{\pm})\,ds_{\pm}^{x}ds_{\pm}^{y} \;\sim\; \mathrm{e}^{-s_{\pm}^{2}/2\mathcal{I}_{\pm}T_S}ds_{\pm}^{x}ds_{\pm}^{y}\,, \tag{8}$$

where $s_{\pm}=(s_{\pm}^{x},s_{\pm}^{y},0)$ is the spin of the normal modes with plus refering to the wriggling modes (having parallel rotations) and minus refering to the bending modes (having opposite rotations). The corresponding moments

of inertia are denoted $\mathcal{I}_\pm$ [19,20]. The degree of fluctuation is governed by the 'spin temperature'

$$T_S = c_S T_{\rm sc} \tag{9}$$

(see Eq. (9)) which can be adjusted by means of the parameter c_S[1]. The fluctuations vanish for $c_S = 0$ so the fragments emerge with the angular momenta dictated by the overall rigid rotation of the scission configuration (which is usually very small for induced fission and entirely absent for spontaneous fission). The default value, $c_S = 1$, leads to $\overline{S}_L \sim 6.2\hbar$ and $\overline{S}_H \sim 7.6\hbar$ for ^{252}Cf(sf) and yields a reasonable agreement with the average energy of photons emitted in fission (see Ref. [20] for details).

After accounting for the total rotational energy of the two fragments, $E_{\rm rot}$, we are left with a total of

$$E_{\rm stat} = E^*_{\rm sc} - E_{\rm rot} \tag{10}$$

for statistical fragment excitation. It is distributed between the two fragments as follows.

First a preliminary partition, $E_{\rm stat} = \acute{E}^*_L + \acute{E}^*_H$, is made according to the heat capacities of the two fragments which are assumed to be proportional to the corresponding Fermi-gas level density parameters, *i.e.*

$$\frac{\acute{E}^*_L}{\acute{E}^*_H} = \frac{a_L}{a_H}\,, \tag{11}$$

where

$$a_i(\acute{E}^*_i) = \frac{A_i}{e_0}\left[1 + \frac{\delta W_i}{U_i}\left(1 - e^{-\gamma U_i}\right)\right]\,, \tag{12}$$

with $U_i = \acute{E}^*_i - \Delta_i$ and $\gamma = 0.05/\text{MeV}$ [13,28]. The pairing energy of the fragment, Δ_i, and its shell correction, δW_i, are tabulated in Ref. [28] based on the mass formula of Koura [29]. The overall scale e_0 is taken as a model parameter but it should be noted that if the shell corrections are negligible, $\delta W_i \approx 0$, or the available energy, U_i, is large, then $a_i \approx A_i/e_0$, *i.e.* a_i is simply proportional to the fragment mass number A_i, and this renormalization is immaterial. We currently assumes the universal value of 10.0724 MeV determined in Ref. [18] for e_0.

If the two fragments are in mutual thermal equilibrium, $T_L = T_H$, the total excitation energy will, on average, be partitioned as above. But because the observed neutron multiplicities suggest that the light fragments tend to be disproportionately excited, the average excitations are modified in favor of the light fragment,

$$\overline{E}^*_L = x\acute{E}^*_L\,,\ \overline{E}^*_H = E_{\rm stat} - \overline{E}^*_L\,, \tag{13}$$

where the adjustable model parameter[2] x is expected be larger than unity. It was found that $x = 1.3$ leads to reasonable agreement with $\nu(A)$ for ^{252}Cf(sf), while $x = 1.2$ is suitable for ^{235}U(n,f) [17].

After the mean fragment excitation energies have been assigned as described above, `FREYA` considers the effect of thermal fluctuations. In Weisskopf's statistical model of the nucleus [30–32], which describes the excited nucleus as a degenerate Fermi gas, the mean excitation of a fragment is related to its temperature T_i by

$$\overline{E}^*_i = a_i(\overline{E}^*_i)T_i^2 \tag{14}$$

and the associated variance in the excitation is

$$\sigma^2_{E_i} = -\frac{\partial^2 \ln \rho_i(E_i)}{\partial E_i^2} = 2\overline{E}^*_i T_i\,. \tag{15}$$

[1] The fissile nucleus dependent parameters cS, alevel0, xeps, c and gmin are specified in file 'inputparameters.dat'.

[2] See footnote 1.

Whereas `FREYA 1.0` sampled an energy fluctuation δE_i^* from a normal distribution of variance $\sigma_{E_i}^2 = 2\overline{E}_i^* T_i$ and adjusted the fragment excitations accordingly, arriving at

$$E_i^* = \overline{E}_i^* + \delta E_i^* \ , \ i = L, H \, , \tag{16}$$

`FREYA 2.0.2` samples an energy fluctuation δE_i^* from a normal distribution of variance

$$c^2 \sigma_{E_i}^2 = 2c^2 \overline{E}_i^* T_i \, , \tag{17}$$

where the factor c multiplying the variance was introduced to explore the effect of the truncation of the normal distribution at the maximum available excitation. It can be adjusted for each fissile nucleus[3]. Its value affects the neutron multiplicity distribution $P(\nu)$ [33]; previous work used the default value, $c = 1.0$.

Energy conservation is accounted for by making a compensating opposite fluctuation in the total kinetic energy [18],

$$\mathrm{TKE} = \overline{\mathrm{TKE}} - \delta E_L^* - \delta E_H^* \, . \tag{18}$$

2.3 Post-fission radiation

After their formation, `FREYA` assumes that the fully accelerated fission fragments first de-excite by sequential neutron evaporation (see Fig. 7), followed by sequential photon emission (see Fig. 8).

2.3.1 Neutron evaporation

Neutron evaporation occurs after the fragments have reached their asymptotic velocities. We treat postfission neutron radiation by iterating a simple treatment of single neutron evaporation until no further neutron emission is energetically possible.

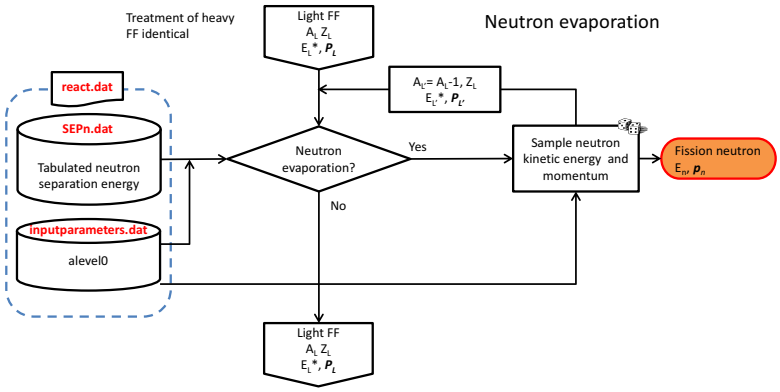

Figure 7: Neutron evaporation.

A fission fragment is an excited nucleus with a total mass equal to its ground-state mass plus its excitation energy, $M_f^* = M_f^{\mathrm{gs}} + E_f^*$. The Q value for neutron emission is then

$$\begin{aligned} Q_n &= M_f^* - M_d^{\mathrm{gs}} - m_n \\ &= M_f^{\mathrm{gs}} + E_f^* - M_d^{\mathrm{gs}} - m_n \end{aligned} \tag{19}$$

[3] See footnote 1.

where $M_d^{\rm gs}$ is the ground-state mass of the daughter nucleus, and m_n is the mass of the ejectile. Using the definition for the neutron separation energy $S_n(Z,A) = -M\left({}^{A}Z\right) + M\left({}^{A-1}Z\right) + m_n$, we have

$$Q_n = E_f^* - S_n(Z,A) \ . \tag{20}$$

The Q value equals the maximum possible excitation energy of the daughter nucleus $Q_n = E_f^{\rm max}$ for vanishing final relative kinetic energy of the ejectile, or when the emitted neutron has no kinetic energy.

Once the Q value is known, it is straightforward to sample the kinetic energy of an evaporated neutron. The evaporated neutrons are assumed to be isotropic (in the frame of the emitting nucleus), apart from a very slight flattening due to the nuclear rotation. Their energy is sampled from a black-body spectrum,

$$\frac{dN_n}{dE_n} \sim E_n \exp(-E_n/T_{\rm max}) \, , \tag{21}$$

where $T_{\rm max}$ is the maximum possible temperature in the daughter nucleus (corresponding to emission of a very soft neutron) and is obtained from

$$a_d T_{\rm max}^2 = Q_n \ , \tag{22}$$

where a_d is the level-density parameter of the daughter nucleus.

The excitation energy of the daughter nucleus is then given by

$$E_d^* = Q_n - E_n \ . \tag{23}$$

FREYA generally assumes that neutron evaporation continues until the nuclear excitation energy is below the threshold $S_n + Q_{\rm min}$, where S_n is the neutron separation energy and $Q_{\rm min} = 0.01$ MeV. Neutron evaporation continues as long as energetically possible. Afterwards, photon emission takes over.

2.3.2 Photon emission

As in FREYA 1.0, neutron evaporation occurs until the nuclear excitation energy of the fission fragments is below the threshold $S_n + Q_{\rm min}$, where S_n is the neutron separation energy and $Q_{\rm min} = 0.01$ MeV. Neutron evaporation continues as long as energetically possible. After neutron evaporation has ceased, the excited product nucleus will undergo sequential photon emission to rid itself of the remaining excitation energy. This energy is both statistical and rotational, see Fig. 5.

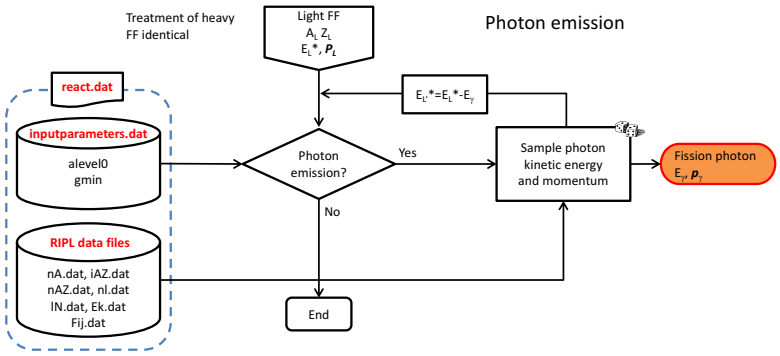

Figure 8: Photon emission.

Photon emission is treated in several stages. Whereas FREYA 1.0 only emitted statistical photons, FREYA 2.0.2 now uses the RIPL-3 data library [34] for the discrete decays towards the end of the decay chain [35].

The first stage — common to FREYA 1.0 and FREYA 2.0.2 — is statistical radiation. These photons are emitted isotropically in the frame of the emitter nucleus with an energy that has been sampled from a black-body spectrum modulated by a giant-dipole resonance (GDR) form factor,

$$\frac{dN_\gamma}{dE_\gamma} \sim \frac{\Gamma_{\rm GDR}^2 E_\gamma^2}{(E_\gamma^2 - E_{\rm GDR}^2)^2 - \Gamma_{\rm GDR}^2 E_\gamma^2} E_\gamma^2 \, {\rm e}^{-E_\gamma/T}, \tag{24}$$

where T, the nuclear temperature prior to emission, is equal to the maximum possible temperature after emission. The position of the resonance is taken as $E_{\rm GDR}/{\rm MeV} = 31.2/A^{1/3} + 20.6/A^{1/6}$ [36], while its width is $\Gamma_{\rm GDR} = 5\,{\rm MeV}$. Each emission reduces the magnitude of the angular momentum by $dS = 1\hbar$. In the statistical radiation of photons, the GDR form factor

$$\frac{\Gamma_{\rm GDR}^2 E_\gamma^2}{(E_\gamma^2 - E_{\rm GDR}^2)^2 - \Gamma_{\rm GDR}^2 E_\gamma^2} \tag{25}$$

is new to FREYA 2.0.2.

In FREYA 1.0, the cascade was continued until the statistical excitation energy available for photon emission was exhausted and the photon energy was below a specified, detector-dependent threshold, $g_{\rm min}$, which is typically fixed at $g_{\rm min} = 100$ keV. FREYA 2.0.2 instead splits the total excitation energy into statistical excitation and rotational energy. After the statistical excitation available for photon emission (when the statistical excitation energy is below the neutron separation energy) is exhausted, the rotational energy must still be disposed of. FREYA 2.0.2 uses the discrete levels in the RIPL-3 library [34] for photon transitions between levels when the photon cascade leads to an energy below any of the tabulated RIPL-3 levels. The RIPL-3 library tabulates discrete electromagnetic transitions for nuclei throughout the nuclear chart. While complete information is available for only relatively few of them, by invoking certain assumptions (see Ref. [35]), it is possible to construct, for each product species, a table of the possible decays to the lowest discrete levels including the level energies ε_l, half lives t_ℓ, and branching ratios. The discrete cascade continues either until the excitation energy is below $g_{\rm min}$, or the half-life t_ℓ, exceeds a specified value $t_{\rm max}$, adjusted to reflect the detector response time [35]. If the photon decay for a particular fragment is not in the RIPL-3 tables, the fragment must still dispose of its rotational energy. In this case, photons are emitted along the yrast line as long as $S > 2$, after which the remaining energy is carried away by a single photon, as described in Ref. [19].

3 FREYA data files

The data files shown in this section are for the most part organized in order of use in the general FREYA sequence of events. Table 1 lists the files used by FREYA.

Upon startup, FREYA reads in a master data file containing

(1) the ZA of the available compound nuclei before fission. There are currently 12 fissionable isotopes: 6 spontaneously fissioning (^{238}U, ^{238}Pu, ^{240}Pu, ^{242}Pu, ^{244}Cm, ^{252}Cf) and 5 neutron-induced (^{233}U, ^{235}U, ^{238}U, ^{239}Pu, ^{241}Pu);

(2) the maximum number of pre-fission neutrons in pre-fission neutron evaporation;

(3) the names of the FREYA data files containing:

   (a) the probability distributions of mass partition $P(A_f)$;

   (b) the pre-equilibrium emission probabilities;

   (c) the pre-equilibrium emission spectra;

Table 1: List of all data files needed by FREYA and the section of the text where they are described. The label *isotope* is a placeholder for the exact compound isotope (just before fission) included, e.g. U236 for the reaction $^{235}\mathrm{U}(n,f)$.

Data file name	Description	Section
react.dat	List of isotopes treated	3.1
SEPn.dat	Neutron separation energy	3.2
fisbar.dat	Nuclei fission barriers	3.3
acorrection.dat	Neutron separation energy	3.4
isotope.xs	Pre-equilibrium emission probability	3.5
isotope.PreEq	Pre-equilibrium emission spectra	3.5.2
Zdis.dat	Charge distribution width	3.6
isotope.Y-Af	Fission fragment yields	3.7.1
gaussfit.dat	Five-Gaussian fit parameters	3.7.2
MassMNMS.dat	Theoretical isotopic mass tables	3.8.1
MassAudi.dat	Experimental isotope mass tables	3.8.2
isotope.TKE-Af	Total kinetic energy	3.9
inputparameters.dat	Fission fragment total excitation energy and partition parameters	3.10
alevel.dat	Shell corrections and pairing effects	3.11
RIPL specific data files		
nA.dat	Number of isotopes for each Z	3.12.1
iAZ.dat	The values of A included for a specified Z	3.12.2
nAZ.dat	The index #N assigned to a given Z,A pair	3.12.3
nl.dat	The number of energy levels in nucleus #N	3.12.4
lN.dat	Points to the array value of the last level of nucleus #N	3.12.5
Ek.dat	Gives the energy and half life of all included levels	3.12.6
Fij.dat	Tabulates all decay branches of all levels	3.12.7

(d) the kinetic energy distributions of the fission fragments.

Because additional isotopes are expected to be regularly added in the future, the code was designed to ease the extension to additional isotopes: algorithm and data are completely separated and isotopes can easily be added by adding lines to the master data file, and generating some of the required files 3a through 3d listed in the enumeration above.

3.1 Master data file react.dat

The master file 'react.dat' contains all of the data files that FREYA uses. It is thus shown in Figs. 1-8. The current version of this file is reproduced below:

```
element  Z   A  reaction  max # pre-fiss n  P(Af) file name  Pre-eq prob  Pre-eq spect  # TKE files  TKE file names
U       92 234   '(n,f)'                3               -      U234.xs    U234.PreEq            1  U234.TKE-Af
U       92 236   '(n,f)'                3               -      U236.xs    U236.PreEq            1  U236.TKE-Af
U       92 238      'sf'                0     U238sf.Y-Af            -             -            1  U238sf.TKE-Af
U       92 239   '(n,f)'                3               -      U239.xs    U239.PreEq            1  U239.TKE-Af
Pu      94 238      'sf'                0     Pu238sf.Y-Af            -             -            1  Pu238sf.TKE-Af
Pu      94 240   '(n,f)'                3               -     Pu240.xs   Pu240.PreEq            1  Pu240.TKE-Af
Pu      94 240      'sf'                0     Pu240sf.Y-Af            -             -            1  Pu240sf.TKE-Af
Pu      94 242   '(n,f)'                3               -     Pu242.xs   Pu242.PreEq            1  Pu242.TKE-Af
Pu      94 242      'sf'                0     Pu242sf.Y-Af            -             -            1  Pu242sf.TKE-Af
Cm      96 244      'sf'                0     Cm244sf.Y-Af            -             -            1  Cm244sf.TKE-Af
Cf      98 252      'sf'                0     Cf252sf.Y-Af            -             -            1  Cf252sf.TKE-Af
```

If this file does not exist, the FREYA fission sampler outputs an error and returns.

Each line in this file corresponds to a compound isotope before fission. Except for the first header line, the overall structure of the master data file is described in Table 2. For neutron-induced fission, one should point

Table 2: Structure of master data file 'react.dat'

Column	Description
element	Symbol of the isotope in the periodic table
Z	Proton number (nuclear charge) of the element
A	Mass number (neutrons + protons) of the *compound* nucleus
reaction	Reaction type, either neutron-induced fission '(n,f)' or spontaneous fission 'sf'
max # pre-fiss n	Maximum number of pre-fission neutrons that this isotope can emit (second, third and fourth chance fission)
$P(A_f)$ file name	Name of the file containing the fission fragment yield probability $P(A_f)$
Pre-eq prob	Name of the file containing the pre-equilibrium emission probability
Pre-eq spect	Name of the file containing the pre-equilibrium emission spectrum
# TKE files	Number of total kinetic energy 'TKE' files that will be read by FREYA
TKE file names	Names of the total kinetic energy files themselves

out that 'A' is the number of nucleons in the compound nucleus, i.e. the nuclear mass number after the incident neutron has been captured by the fissile isotope. Thus the first line corresponds to the neutron-induced fission reaction $n+^{233}$U.

If a filename specified in 'react.dat' does not exist, FREYA outputs an error and returns. When a hyphen '-' replaces a filename, FREYA uses a default treatment, as described later.

3.2 Neutron separation energy in file SEPn.dat

As explained in Sec. 2, the neutron separation energy is used for multiple purposes. It is used to calculate the excitation energy of the nucleus after absorption of the incident neutron (see Fig. 1) for neutron-induced fission. It determines whether pre-fission evaporation (see Fig. 2) is possible: as long as the excitation energy of the compound nucleus exceeds the neutron separation energy S_n, one or more neutrons can be emitted before fission. It is used to determine the kinetic energy of the evaporation neutrons (see Fig. 7). For a fragment of statistical excitation E^*, the maximum temperature in its evaporation daughter, $T_{\max}$, is obtained from $aT_{\max}^2 = E^* - S_n(Z,A)$. The neutron kinetic energy E_n is sampled from $f_n(E_n) \sim E_n \exp(-E_n/T_{\max})$. Finally, it is used to calculate how many prompt neutrons are emitted by the fission fragments. Neutron evaporation ceases when the statistical excitation energy $E^* < S_n(Z,A) + Q_{\min}$, i.e. neutrons are emitted as long as the Q value for emission exceeds $Q_{\min}$, at which point photon emission takes over.

This file contains the neutron separation energy for different fissile isotopes and is used to decide whether pre-fission neutron evaporation takes place. An excerpt of the data file "SEPn.dat" is shown below:

```
 Z    A   separation energy [keV]
92  218            8847.36
92  219            6782.61
(...)
98  255            4603.
98  256            5841.
```

Except for the first header line, the overall structure of this data file is explained in Table 3.

Table 3: Structure of data file 'SEPn.dat'

Column	Description
Z	Proton number
A	Mass number
separation energy	Neutron separation energy in units of keV

3.3 Data file `fisbar.dat`

The data file "fisbar.dat" is used in Fig. 2 showing pre-fission evaporation, and contains fission barriers of nuclei. The role of fission barriers is explained in Sec. 2.1.2. If a nucleus is not in the table, a default fission barrier of 0 MeV is used.

Fission barriers are used to compute the decay width of fission. The criterion for pre-fission evaporation is not whether it is energetically possible ($E^* > S_n$), as in neutron evaporation explained in Sec. 2.3.1. Rather, a choice is made based on $\Gamma_n(E^*)/\Gamma_\mathrm{f}(E^*)$, the relative magnitudes of the decay widths. Of course, $\Gamma_n(E^*)$ vanishes for E^* below S_n.

An excerpt of data file "fisbar.dat" is shown below:

```
 Z   A  fiss. barrier [MeV]
92 231           5.5
92 232           5.4
(...)
94 245           5.85
94 246           5.4
```

Except for the first header line, the structure of this data file is explained in Table 4.

Table 4: Structure of data file 'fisbar.dat'

Column	Description
Z	proton number
A	mass number
fiss. barrier	fission barrier in units of MeV

3.4 Data file `acorrection.dat`

Similarly to data file 'fisbar.dat', "acorrection.dat" is used in Fig. 2 for pre-fission evaporation and contains correction factors for the level-density parameters of a few isotopes of uranium and plutonium.

As is common, `FREYA` assumes nuclei level densities to be of the form $\rho\left(E_i^*\right) \sim \exp(2\sqrt{a_i U_i})$, where U_i is the effective statistical energy and a_i is the level-density parameter. Level-density parameters enter in the calculation of $\Gamma_n(E_i^*)$ and $\Gamma_\mathrm{f}(E_i^*)$, the neutron evaporation and fission decay widths [23]. For a few isotopes of uranium and plutonium, the level-density parameters a_i are multiplied by correction factors a_n and a_f for these calculations.

The data file "acorrection.dat" is reproduced below in its entirety:

```
 Z   A  an correction factor  af correction factor
92 236                 1.03                 0.96
92 235                 1.14                 1.20
92 234                 1.00                 1.00
94 240                 1.00                 1.00
94 239                 0.92                 1.00
94 238                 1.00                 1.00
```

Except for the first header line, the overall structure of the data file 'acorrection.dat' is explained in Table 5.

Table 5: Structure of data file 'acorrection.dat'

Column	Description
Z	Proton number
A	Mass number
a_n	Correction to level-density parameter used to compute neutron evaporation decay width, Γ_n
a_f	Correction to level-density parameter used to compute fission decay width, $\Gamma_{\rm f}$

3.5 Data files associated with pre-equilibrium neutron emission

In pre-equilibrium neutron emission, an incident neutron interacts with the fissile nucleus and is re-emitted afterwards before the nucleus fissions. It is different from multichance fission, where a neutron other than the incident neutron is emitted before fission. Files with pre-equilibrium emission probabilities and pre-equilibrium energy spectra are used in the algorithm for pre-equilibrium neutron emission, see Fig. 1.

In file 'react.dat' ^{234}U*, ^{236}U*, ^{239}U*, ^{240}Pu* and ^{242}Pu* have pre-equilibrium emission probabilities and energy spectra. For a given isotope, both the pre-equilibrium emission probability and the energy spectrum are necessary. If one is given and the other is missing, the `FREYA` fission sampler will return with an error message.

3.5.1 Pre-equilibrium emission probabilities

The excerpt of file 'U236.xs' below shows the probability of pre-equilibrium neutron emission from the compound nucleus ^{236}U as a function of the incident neutron energy E_{in}:

```
 U-236.xs: Probability for pre-equil emission vs Ein:
  100   0.20000
    0   0.00000 0.0000000E+00
    1   0.20000 0.0000000E+00
    2   0.40000 0.0000000E+00
    3   0.60000 0.0000000E+00
    4   0.80000 0.0000000E+00
    5   1.00000 0.6432276E-04
    6   1.20000 0.2734767E-03
    7   1.40000 0.6399593E-03
(...)
   99  19.80000 0.2314241E+00
  100  20.00000 0.2336182E+00
```

The overall structure of the data file, from line 3 on, is described in Table 6. The first two lines are header lines. Line 1 is an identifying comment. Line 2 has two entries: *a*) The total number of data entries in the file "minus

Table 6: Structure of pre-equilibrium emission probability data file

Column	Description
1	Entry number
2	Incident neutron energy, E_n, in units of MeV
3	Probability of pre-equilibrium neutron emission for incident energy E_n, $P(p_\pi, h_\pi, p_\nu, h_\nu)$ in Eq. (1)

one". (In this case, the file has 101 data entries; thus the first number on line 2 is 100); *b*) The width of the energy bins in units of MeV. (The bin width is 0.2 MeV in this file.)

For the compound nucleus ^{236}U, we read in file "U236.xs" that the probablity for pre-equilibrium neutron emission is null for neutron incident energies from 0 to 0.8 MeV.

3.5.2 Pre-equilibrium emission spectra

An example of the neutron spectrum from pre-equilibrium emission is shown below as a function of E_{in}. These lines are taken from file 'U236.PreEq' for the compound nucleus ^{236}U:

```
Pre-equilibrium neutron spectra from U236* for various En (.PreEq):
  100 incident neutron energies En in steps of   0.200 MeV:
    0   0.000    0  0.199153
    1   0.200    0  0.199153
    2   0.400    0  0.199153
    3   0.600    0  0.199153
    4   0.800    0  0.199153
    5   1.000    1  0.199153
  0.199153 0.2510638E+01
    6   1.200    2  0.199153
  0.199153 0.3564677E+01
  0.398305 0.1456601E+01
    7   1.400    3  0.199153
  0.199153 0.1674361E+01
  0.398305 0.2424930E+01
  0.597458 0.9219841E+00
(...)
  100  20.000   96  0.199153
  0.199153 0.1114254E-01
  0.398305 0.2194049E-01
  0.597458 0.2977476E-01
(...)
 18.720339 0.6576045E-02
 18.919493 0.4754821E-02
 19.118645 0.1891974E-02
```

Except for the first two header lines, the overall structure of the data file for the pre-equilibrium neutron emission spectrum is explained in Tables 7 and 8. The structure description in Table 7 applies to lines 3-8, 10, 13, etc. of file "U236.PreEq" shown above. For the other lines, the structure description in Table 8 applies.

The file "U236.PreEq" gives the emission spectrum out to its kinematic endpoint. The entry numbers and incident neutron energies are the same as those in the first two columns of the probability distribution, as described in Table 7. If the third entry in "U236.PreEq" is 0, there are no emission spectrum entries since there

Table 7: Structure of pre-equilibrium emission spectrum data file

Column	Description
1	Entry number (Same as Column 1 in Table 6.)
2	Incident neutron energy, E_n, in units of MeV. (Same as Column 1 in Table 6.)
3	Number of entries in the pre-equilibrium neutron energy spectrum
4	Bin width of the pre-equilibrium energy spectrum in units of MeV. (Identical for all entries.)

is zero probability for emission. If this entry is nonzero, the emission spectrum follows with a number of entries equal to the integer value of Column 3. Table 8 describes these entries.

Table 8: Description of pre-equilibrium emission spectrum for each incident neutron energy where the number of entries in the third column of Table 7 is not null.

Column	Description
1	Pre-equilibrium emission neutron energy.
2	Pre-equilibrium emission neutron spectrum, $d\sigma_n/dE$ in Eq. (1), normalized to unity.

The number of data points and the width of the incident neutron energy bins in the pre-equilibrium emission probability and the energy spectrum files must match.

3.6 Data file `Zdis.dat`

The data file 'Zdis.dat" is used to sample the fission fragment charge partition, see Fig. 3. It contains the standard deviation σ_Z in Eq. (3) for few elements with $220 \leq A \leq 260$. An excerpt of the file is shown below:

```
  A  charge distribution
220                0.38
221                0.38
(...)
259                0.47
260                0.47
```

The overall structure of the data file 'Zdis.dat', aside from the first header line, is explained in Table 9.

Table 9: Structure of data file 'Zdis.dat'

Column	Description
A	Mass number
σ_Z	Width of charge distribution, standard deviation in Eq. (3)

3.7 Data files for fission fragment yields

In cases where either data on only a single incident energy is available or for some spontaneously fissioning isotopes, the fragment yields are sampled from a single data file. The structure of these data files are described

in Sec. 3.7.1. In other cases, a five-Gaussian fit to the fragment yields has been made. The structure of the data file contaning the fit parameters, 'gaussfit.dat', is described in Sec. 3.7.2. (Both single data files and five-Gaussian fits are available for spontaneous fission. In general the data file is used for sampling in these cases.) When the full incident neutron energy dependence of the yields is required for energies up to $E_n = 20$ MeV, an energy dependence of the Gaussian fits has been developed, as discussed in Sec. 3.7.2.

3.7.1 Data files for single fission fragment yields $P(A_f)$

The data files for single energy or spontaneous fission fragment yields $P(A_f)$ are used in the selection of the fission fragment mass numbers, see Fig. 3. The excerpt of the file 'U238sf.Y-Af' below shows $P(A_f)$ for spontaneous fission of the nucleus ^{238}U in 'react.dat'.

```
P(Af) for 238U(sf) [Ivanov, INT]
 81    0.1165
 82    0.1745
(...)
156    0.1144
157    0.0513
  0    0.00
```

Aside from the first header line, the lines of the $P(A_f)$ files are described in Table 10. The fragment yields

Table 10: Structure of fission product yield probability data file $P(A_f)$

Column	Description
1	Fragment mass number, A_f
2	Fragment yields $P(A_f)$
3	Uncertainty on $P(A_f)$, when available

$P(A_f)$ do not need to be normalized, the code normalizes them automatically. The header line indicates the origin or author of the data, e.g. "Ivanov". The end of the data file is identified by a line where the fragment mass number A_f is 0.

3.7.2 Data file `gaussfit.dat`

When the file name for the fission fragment yield $P(A_f)$ is replaced by a hyphen '-' (e.g. ^{236}U* and ^{240}Pu* in file 'react.dat'), `FREYA` samples the fission products from a five-Gaussian fit to the fission product yield distributions. The fits are isotope and energy dependent, as is now described.

The mass yields $Y(A_f)$ of the fission fragments for a given neutron energy E_n are composed of three distinct Gaussian modes,

$$Y(A_f) \;=\; G_1(A_f) + G_2(A_f) + G_0(A_f)\;. \tag{26}$$

The first two terms represent asymmetric fission modes associated with the spherical shell closure at $N = 82$ and the deformed shell closure at $N = 88$, respectively. The last term is a symmetric mode. While this mode is small at low excitation energies, its importance increases with excitation energy.

The asymmetric modes are composed of two Gaussians,

$$G_i = \frac{C_{ni}}{\sqrt{2\pi}W_{ni}}\left[\exp\left(-\frac{(A_f-\overline{A}-D_{ni})^2}{2W_{ni}^2}\right)+\exp\left(-\frac{(A_f-\overline{A}+D_{ni})^2}{2W_{ni}^2}\right)\right], \tag{27}$$

where $i = 1,2$ while the symmetric mode is given by a single Gaussian

$$G_0 = \frac{C_{n0}}{\sqrt{2\pi}W_{n0}} \exp\left(-\frac{(A_f - \overline{A})^2}{2W_{n0}^2}\right) , \tag{28}$$

with $\overline{A} = A_0/2$.

The values of D_{ni} are displacements that are anchored above the symmetry point by the spherical and deformed shell closures. Because these occur at specific neutron numbers, $D_n(i)$ are energy independent. The values of $D_n(i)$ are smaller for ^{240}Pu* than ^{236}U* due to the larger value of A_0 for Pu.

The widths of the asymmetric Gaussians are assumed to be energy dependent and are expended to second order in neutron energy,

$$W_{ni} = W_n(i,0) + W_n(i,1)E_n + W_n(i,2)E_n^2 . \tag{29}$$

The width of the symmetric Gaussian is assumed to be energy independent.

The energy dependence of the normalization coefficients C_{n1} and C_{n2} is given as

$$C_{ni} = C_n(i,0)\,(1 + \exp[(E_n - C_n(i,1))/C_n(i,2)])^{-1} . \tag{30}$$

Since each event leads to two fragments, the yields are normalized so that $\sum_{A_f} Y(A_f) = 2$. Thus,

$$2C_{n1} + 2C_{n2} + C_{n0} = 2 , \tag{31}$$

apart from a negligible correction because A_f is discrete and bounded from both below and above. Therefore, C_{n0} is determined from Eq. (31) at each value of E_n.

Finally, we note that, above the threshold for pre-fission neutron evaporation, the yields include contributions from first-chance fission and higher. For more information, see Ref. [18].

The list of parameters used for the gaussian fits are in the file 'gaussfit.dat', reproduced below. The structure of 'gaussfit.dat' is described in Table 11.

```
Weight of each fission mode
 Z   A    Cn(1,0)  Cn(1,1)  Cn(1,2)
          Cn(2,0)  Cn(2,1)  Cn(2,2)
            Dn(1)    Dn(2)
          Wn(0,0)  Wn(0,1)  Wn(0,2)
          Wn(1,0)  Wn(1,1)  Wn(1,2)
          Wn(2,0)  Wn(2,1)  Wn(2,2)
92 234    0.948      9.169      1.1887
          0.04095    9.169      1.1887
         21.57      14.02
         12.01       0.0        0.0
          5.976      0.09376    0.034
          2.896      0.1106     0.008
92 236    0.7706     9.169      1.1887
          0.2191     9.169      1.1887
         22.91      16.08
         12.0        0.0        0.0
          5.183      0.09376    0.034
          3.597      0.1106     0.008
92 238    0.494508   1.0        0.05
          0.505472   1.0        0.05
         25.81      18.22
          4.832      0.0        0.0
          3.256      0.0        0.0
          3.313      0.0        0.0
```

```
92 239   0.716110  16.91       0.9928
         0.283748  16.91       0.9928
        21.966     15.177
        13.34       0.0        0.0
         5.825      0.0        0.01471
         3.175      0.0587     0.0
94 240   0.74      10.14       1.15
         0.253     10.14       1.15
        21.0       14.83
        12.0        0.0        0.0
         6.24534    0.09376    0.034
         3.66784    0.1106     0.008
94 242   0.6592    10.14       1.15
         0.3407    10.14       1.15
        20.38      14.44
        11.91       0.0        0.0
         5.664      0.09376    0.034
         3.231      0.1106     0.008
96 244   0.41987    1.0        0.05
         0.580064   1.0        0.05
        21.04      15.12
         0.7404     0.0        0.0
         5.542      0.0        0.0
         3.692      0.0        0.0
98 252   0.655921   1.0        0.05
         0.344077   1.0        0.05
        18.02      15.78
        14.01       0.0        0.0
         7.106      0.0        0.0
         5.546      0.0        0.0
```

Table 11: Structure of fission product yield probability data file 'gaussfit.dat'

Section	Line#	Description
Header	1	Descriptive file header
	2-3	The first two variables on line 2 are the proton number Z and mass number A of the compound nucleus before fission. This isotope must be present in the file 'react.dat'. The three parameters $C_n(i,j)$ on lines 2 and 3 describe the energy dependence of the normalization coefficients, see Eq. (30). While $C_n(i,0)$ is a number, $C_n(i,1)$ and $C_n(i,2)$ have units of MeV. The normalization of the symmetric mode is constructed from Eq. (31).
	4	The energy-independent values $D_n(i)$ are the centroid shifts of the asymmetric fission modes.
	5-7	The parameters $W_n(i,j)$ are the energy-dependent widths of the Gaussians describing the asymmetric fission modes, see Eq. (29). While $W_n(i,0)$ is dimensionless, $W_n(i,1)$ and $W_n(i,2)$ have units of MeV^{-1} and MeV^{-2} respectively.
Data	Each subsequent set of 6 lines corresponds to the five-Gaussian fit parameters for the indicated Z A combination. Spontaneous fission has no energy dependence. Therefore, $W_n(i,1) = W_n(i,2) = 0$ while $C_n(i,1) \equiv 1$ and $C_n(i,2) \equiv 0.05$ so that $C_{ni} \sim C_n(i,0)$ in Eq. (30).	
	8-13	Gaussian fit parameters for first Z A combination
	14-19	Gaussian fit parameters for second Z A combination
	20-35	(...)

3.8 Isotopic mass tables

The isotope mass tables used in the scission algorithm in Fig. 4 are described here. When available, the experimental measurements in 'MassAudi.dat' are used. Otherwise, the theoretical values in 'MassMNMS.dat' are used.

The structure of the two files is essentially identical. Both files have a five-line header, including two equations, identifying the components of the file. The first equation of the five-line header gives the ground state mass of the nucleus,

$$M(Z,A) = Au + D(Z,A) \ , \tag{32}$$

where Au is the mass number times the atomic mass unit, and $D(Z,A)$ is the mass defect, all in units of MeV. The numerical value for u is given in the third line of the header file, also in units of MeV. The second equation, on the fourth line of the header, defines the nuclear binding energy

$$B(Z,A) = ZD(H) + ND(n) - D(Z,A) \ . \tag{33}$$

The binding energy of the compound nucleus is the difference between the sum of the mass defects for all nucleons and the mass defect of the compound nucleus.

The structure of the data in these files following the header is explained in Table 12. To indicate the end of the data files, the last line of the file has five zero values.

Table 12: Structure of data files 'MassMNMS.dat' and 'MassAudi.dat'

Column	Description
Z	Proton number
A	Mass number
M	Ground state isotopic mass in units of MeV
D	Mass defect in units of MeV
B	Binding energy in units of MeV

3.8.1 Theoretical isotopic mass tables in data file `MassMNMS.dat`

The theoretical isotopic masses, mass defects and binding energies are taken from Möller *et al.* [27]. The excerpt from the file 'MassMNMS.dat' shows some of the theoretical masses. Note that the lowest tabulated theorietical mass is for ^{16}O, $Z = 8, A = 16$.

```
 * Theoretical masses from MNMS 1995:
 * M(Z,A) [MeV] = A*u + D(Z,A) where u is
  931.493835 MeV
 * B(Z,A) = Z*D(H) + N*D(n) - D(Z,A)
 *  Z    A      M(MeV)       D(MeV)       B(MeV)
    8   16   14899.0615     -4.84000    127.72232
    8   17   15835.2256     -0.17000    131.12367
(...)
  120  299  278729.9688    213.32001   2106.12451
  120  300  279662.2812    214.14000   2113.37573
    0    0       0.0000      0.00000      0.00000
    0    0       0.0000      0.00000      0.00000
```

3.8.2 Experimental isotopic mass tables in data file `MassAudi.dat`

This table contains the experimentally measured isotopic masses, mass defects and binding energies published by Audi and Wapstra [26]. Whenever available, the experimental values will override the theoretical ones in Sec. 3.8.1. An excerpt of this file is shown below. Note that the neutron ($Z = 0$, $A = 1$) and proton ($Z = 1$, $A = 1$) are the first two entries in this table.

```
 * Audi & Wapstra NPA595 (1995) 409:
 * M(Z,A) [MeV] = A*u + D(Z,A) where u is
  931.493835 MeV
 * B(Z,A) = Z*D(H) + N*D(n) - D(Z,A)
 *  Z    A      M(MeV)       D(MeV)       B(MeV)
    0    1     939.5652      8.07135      0.00000
    1    1     938.7828      7.28894      0.00000
(...)
  117  292  272189.5312    193.33130   2071.96094
  118  293  273127.6562    199.96246   2072.61865
    0    0       0.0000      0.00000      0.00000
```

3.9 Total kinetic energy data file

`FREYA` needs to read in the total kinetic energy TKE data files, given as a function of the heavy fragment mass A_H. One or more TKE files per isotope are allowed. The number of TKE files for a given isotope is specified in the field '# TKE files' in 'react.dat'. When multiple TKE files are entered, the code calculates the average of the experimental TKE values for each A_H, counting each data point equally. (Therefore A_H and $A_L = A_0 - A_f$ count equally). An entry of 0 in the field '# TKE files' is invalid because there is no default behavior for the total kinetic energy data. If the TKE data file is missing or invalid, `FREYA` will generate an error message.

The total kinetic energy data files are used in the algorithm for the selection of fission fragment energies, see Fig. 5 and Eq. 5. An example of a TKE file is shown below for neutron-induced fission of ^{235}U, for the compound nucleus ^{236}U*:

```
 TKE(Af) for 236U(n,f) [Nishio]:
   78  158
   78  148.0319
   79  149.8098
(...)
  157  149.8098
  158  148.0319
```

The first line indicates the compound nucleus and the origin or author of the data, e.g. "Nishio".

Table 13: Structure of total kinetic energy data file

Column	description
A_H	Mass number of heavy fission fragment
TKE	Total kinetic energy in units of MeV, Eq. 5

3.10 Data file `inputparameters.dat`

`FREYA` contains a number of adjustable parameters that control various physics aspects. File 'inputparameters.dat' contains the parameters used to calculate the total excitation energy of the fission fragments and

partition the excitation energy between the two fragments (see Eqs. (5)-(17) in Sec. 2). This file enters into the algorithm for the selection of fission fragment energies (Figs. 5-6) and the algorithm for the neutron evaporation and photon emission (Figs. 7-8).

This file also includes the parameter dTKE which shifts the TKE globally to get agreement with the measured average neutron multiplicity, $\overline{\nu}$. If a hyphen '-' is given in the field 'dTKE file name' or if this field is empty, FREYA uses the energy-independent value specified in the next field 'dTKE'. An entry in the column 'dTKE file name' is only expected for neutron-induced fission at multiple energies, for E_n up to 20 MeV.

If isotopes in file 'react.dat' have no entries in file 'inputparameters.dat', the unspecified fields take the species-independent default values listed in Table 14.

```
  Z   A  reaction   alevel0  xeps  c    cS   gmin   dTKE file name   dTKE
92  234   '(n,f)'   10.37    1.15  1.2  0.87 0.150  U234.dTKE        0.39
92  236   '(n,f)'   10.37    1.15  1.3  0.87 0.150  U236.dTKE        0.39
92  238   'sf'      10.0724  1.2   0.92 0.87 0.150  -               -1.34541
92  239   '(n,f)'   10.37    1.15  1.2  0.87 0.150  U239.dTKE        1.1
94  238   'sf'      10.0724  1.2   1.91 0.87 0.150  -               -1.3657
94  240   '(n,f)'   10.37    1.15  1.2  0.87 0.150  Pu240.dTKE       1.1
94  240   'sf'      10.0724  1.3   3.0  0.87 0.150  -               -3.07119
94  242   '(n,f)'   10.37    1.15  1.2  0.87 0.150  Pu242.dTKE       1.1
94  242   'sf'      10.0724  1.1   3.4  0.87 0.150  -               -1.59993
96  244   'sf'      10.0724  1.2   1.34 0.87 0.150  -               -4.35
98  252   'sf'      10.37    1.27  1.18 0.87 0.150  -                0.52
```

3.11 Data file `alevel.dat`

The file 'alevel.dat' contains the values δW and Δ in Eq. (12) which are used to include shell corrections and pairing effects in the level-density parameter a_i (see function 'alevel' in FORTRAN code). The data is this file enter whenever the level density is used, not only when dividing the statistical excitation between the two fragments but also when sampling the energy of an emitted neutron or photon. The flow charts indicate that 'alevel.dat' is used to determine fission fragment rotational energies and thermal fluctuations (see Figs. 5-6) as well as for neutron evaporation and photon emission (Figs. 7-8). An excerpt of file 'alevel.dat' is shown below.

```
   Z    A   deltaW    Delta  [notes at end of file]
  18   57   1.58       1.68942
  18   58   1.73       2.48275
(...)
  98  251   0.00       0.00
  98  252   0.00       0.00
   0    0   0.00000    0.00000
   Z    A   deltaW    Delta
(...)
```

Aside from the first header line and the last comment lines, the overall structure of the data in this file is described in Table 15. The data file 'alevel.dat' must contain values of Z, A, δW, Δ in order of uninterrupted, increasing Z. The values for each Z in order of uninterrupted, increasing A are nested within the increasing Z values. Of the 7090 current entries, 7050 entries are from Koura [29]. Twenty-six entries for $Z = 18$ (8), $Z = 19$ (7) and $Z = 94$ (11) were added for ^{239}Pu(n,f). For these extra entries, the shell energy δW was taken to be $E_{\rm mic}$, the microscopic (pairing and shell) part of the nuclear potential energy of deformation, from Ref. [27], while the pairing energy Δ was extrapolated from nearby values already in the table. Five entries were added for $Z = 96$ and seven entries for $Z = 98$. For these twelve entries, zeros were used for δW and Δ because the values are not experimentally accessible and there is no need for refined values. Finally, δW and Δ values were

Table 14: Structure of data file 'inputparameters.dat'

Column	Description	default value
Z	Proton number	
A	Mass number of compound nucleus	
reaction	Reaction type, either neutron-induced fission '(n,f)' or spontaneous fission 'sf'	
alevel0	Asymptotic level density parameter e_0 (see Eq. (12) and Ref. [18]), e_0 is the overall scale of the Fermi-gas level density parameters	10.0724 MeV^{-1}
xeps	Parameter for asymmetric distribution of excitation energy between the light and heavy fragments (see Eq. (13)), the advantage in excitation energy given to the light fragment	1.23389
c	parameter to control relative width of normal distribution sampled to calculate thermal fluctuations in the fission fragments (see Eq. (17))	1.
cS (formerly cTS)	the ratio of the 'spin temperature' to the 'scission' temperature (see Eq.(9))	1.
gmin	The detection threshold for photons in FREYA (detector dependent). Photons with energies below this threshold are not counted in the multiplicity.	0.1 MeV
dTKE file name	Name of file containing $d\mathrm{TKE}(E_n)$ (see Eq. (5)).	
dTKE	an overall shift of $\overline{\mathrm{TKE}}$ relative to the input TKE(A), used to adjust the average neutron multiplicity $\overline{\nu}$ (see Eq. (5))	1.53729 MeV

added for ^{241}Pu and ^{242}Pu. The line following the last data line is identified by at least four numbers, the first one of which must be $Z = 0$.

Table 15: Description of structure for data file 'alevel.dat'

column	notation	meaning
1	`Z`	Proton number
2	`A`	Mass number
3	`deltaW`	Shell correction δW (see Eq. (12))
4	`Delta`	Pairing energy Δ (see Eq. (12))

Beware that the maximum number of entries in that file is currently set to 7090.

3.12 Data files for RIPL-3 photon decays

The RIPL-3 [34] photon decay levels have been added to `FREYA`. The RIPL-3 libraries have been modified for fast searches to suit `FREYA`'s needs. The data files needed for implementation of these libraries are discussed in

this subsection.

3.12.1 Data file `nA.dat`

The data file `nA.dat` lists the number of isotopes (*i.e.* A values) for each element (*i.e.* Z value) included from the RIPL-3 tables. The first several and the last few lines of `nA.dat` are shown below:

```
nA(Z): Number of isotopes for each Z
    8   80: minZ & maxZ
    8    6
    9    7
(...)
   79   21
   80   27
```

The first line is a descriptor: `nA(Z)` is the number of isotopes included for an element with charge Z. The second line gives the minimum and maximum values of Z for the elements included. he remainder of the data file `nA.dat` lists the number of isotopes included for each element (see Table 16).

Table 16: Description of the data on the file `nA.dat`

column	notation	meaning
1	`Z`	Nuclear charge number Z
2	`nA`	Number of mass numbers A for this Z

3.12.2 Data file `iAZ.dat`

The data file `iAZ.dat` gives the mass number A of isotope #m for element Z. The first several and the last few lines of `iAZ.dat` are shown below:

```
iAZ(Z,m): Mass numbers for each Z
    8   80: minZ & maxZ
    8    1   15
    8    2   16
(...)
   80   26  204
   80   27  205
```

The first line is a descriptor: `iAZ(Z,m)` is the mass number of included isotope number `m` for the element with charge number `Z`. The second line gives the minimum and maximum values of `Z` for the elements included. The remainder of the data file `iAZ.dat` lists the mass numbers for each included nuclide (see Table 17). For a given Z, the first (and smallest) included A value is $A_{\min}(Z) = \texttt{iAZ}(\texttt{Z},1)$ and the last (and largest) included A value is $A_{\max}(Z) = \texttt{iAZ}(\texttt{Z},\texttt{nA}(\texttt{Z}))$. But not all the intermediate A values are necessarily included, isotopes that have no excited levels contribute no decay lines and are omitted (such passive isotopes have index zero, see Sec. 3.12.3 below).

3.12.3 Data file `nAZ.dat`

The data file `nAZ.dat` gives the sequential index $N(Z,A)$ for each included nuclide with mass number A and charge number Z for the elements included. The first several and the last few lines of `nAZ.dat` are shown below:

Table 17: Description of the data on the file `iAZ.dat`

column	notation	meaning
1	`Z`	Nuclear charge number Z
2	`m`	Number of included isotope for this Z (`m=1,...,nA(Z)`)
3	`A`	Mass number A for included isotope #m of element Z

```
Index for nucleus (Z,A)
    8   80: minZ & maxZ
    8    1    1
    8    2    2
(...)
   80   27 1304
   80   28 1305
```

The first line is a descriptor: this file defines the index $N(Z,A)$ for each included nuclide ${}^{A}Z$. The second line gives the minimum and maximum values of Z for the elements included. The remainder of the data file `nAZ.dat` lists the global index for each considered nuclide (see Table 18). The included nuclides are indexed

Table 18: Description of the data on the file `nAZ.dat`

column	notation	meaning
1	`Z`	Nuclear charge number Z
2	`j`	Isotope counter for this Z (`j=1,...,Amax(Z)-Amin(Z)+1`)
3	`N(Z,A)`	Index for the nuclide ${}^{A}Z$

sequentially, with the first being $N(8,15) = 1$ and the last being $N(80,205) = 1197$. Thus the nuclide ${}^{A}Z$ has the index $N(Z,A) = \texttt{nAZ}(\texttt{i},\texttt{j})$ with $i = Z$ and $1 \le j \le A_{\max}(Z) - A_{\min}(Z) + 1$ with $A_{\min}(Z) = \texttt{iAZ}(\texttt{Z},1)$ and $A_{\max}(Z) = \texttt{iAZ}(\texttt{Z},\texttt{nA}(\texttt{Z}))$. Note that $A_{\max}(Z) - A_{\min}(Z) + 1$ may exceed `nA(Z)` because a nuclide ${}^{A}Z$ for which only the ground state is in the RIPL-3 table contributes no photon lines and is omitted, with the corresponding index `N(Z,A)` being set to zero. [The first such example occurs for ${}^{35}P$ which has `i=15` and `j=7`.]

3.12.4 Data file `nl.dat`

The data file `nl.dat` gives the number of energy levels included for each of the included nuclides (*i.e.* those whose index is positive). The first several and the last few lines of `nl.dat` are shown below:

```
nl(N): Number of energy levels in nucleus #N
 1305: Number of Nuclei
   44    1    8   15
   29    2    8   16
(...)
   35 1304   80  204
    9 1305   80  205
```

The first line is a descriptor: this file gives the number of energy levels included for nucleus #N. The second line indicates the total number of included nuclides (*i.e.* those having photon lines). The remainder of the data file `nl.dat` lists the number of levels for each included nuclide (see Table 19). The data `nl.dat` file does not

Table 19: Description of the data on the file `nl.dat`

column	notation	meaning
1	n_{levels}	Number of levels included for nuclide #N;
2	#N	its index $N(Z,A)$;
3	Z	its charge number;
4	A	its mass number

include nuclides for cases where only ground state nuclei are included in the RIPL-3 table (so, occasionally, for a given Z, the mass number A is not sequential).

3.12.5 Data file `lN.dat`

All the contributing levels are stored sequentially into one large array and the data file `lN.dat` points to the location of the last level of the each included nuclide. The first several and the last few lines of `lN.dat` are shown below:

```
lN(N) points to the last level of nucleus #N
 1305: Number of Nuclei
    0         0
    1        44
(...)
 1304     38165
 1305     38174
```

The first line is a descriptor: the array `lN(N)` points to the location of the last level of each included nuclide, starting with `lN(0)=0` and `lN(1)=nl(1)`; generally we have `lN(N)=lN(N-1)+nl(N)`. There are a total of 35494 contributing levels (last line).

Table 20: Description of the data on the file `lN.dat`

column	description	notation
1	`N`	Index of an included nucleus
2	`lN(N)`	Location of the last level in the nuclide #N

3.12.6 Data file `Ek.dat`

The data file `Ek.dat` lists the energy of the photons emitted from the included levels for each of the included nuclides. The first several and the last few lines of `Ek.dat` are shown below:

```
E(l,N) & nk(l,N) & t(N,l):
     38174: Number of levels
         1  0.000000         0         0   1.22E+02
         2  5.183000         1         1   5.70E-15
(...)
     38173  1.447500         1    277375   0.00E+00
     38174  1.556400         2    277377   1.09E-03
```

The first line is a descriptor of the three characteristics of a level (N,ℓ): its excitation energy, $E(N,\ell)$, the number of possible decays from that level, $n_\gamma(N,\ell)$, and the associated half-life, $t(N,\ell)$. Thus the number of lines in `Ek.dat` following line 2 is the number of included levels, 35494.

Table 21: Description of the data on the file `Ek.dat`

column	notation	meaning
1	$L(N,\ell)$	Index of level ℓ in nucleus #N;
2	$E(N,\ell)$	energy of the level (MeV);
3	$n_\gamma(N,\ell)$	number of decays from the level;
4	$k(N,\ell)$	location of last decay from the level;
5	$t(N,\ell)$	half-life of the level (seconds)

The RIPL-3 levels that are included in the tables have been renumbered as necessary to ensure that they appear according to increasing energy. Because the energy is given relative to the ground state, the first tabulated level for each nuclide is always zero. In any given nuclide, some levels may have the same energy, but they will generally not have the same half-life.

Each included level (N,ℓ) has $n_\gamma(N,\ell)$ possible decays identified by $k = 1, n_\gamma$, except for the ground state which has $n_\gamma(N,1) = 0$. The information on these decays, the final levels and the branching ratios, is stored sequentially into a combined arrays and $k(N,\ell)$ points to the location of the last decay from the level ℓ in the nuclide #N. Thus the value of $k(N,\ell)$ for the last decay branch from the highest included level ℓ in the last included nuclide #N equals the total number of different decays included, 266950.

The half-life of a level is given, if known. If not, it is given as zero in the data file, while a negative value, -1, indicates that the level is stable.

3.12.7 Data file `Fij.dat`

The data file `Fij.dat` provides the information needed for `FREYA` to make the selection between the different competing decay branches during the final cascade through the discrete levels.

The beginning of `Fij.dat` is shown below:

```
nf & Fij:
    277377: Number of decays
          1          0         44 :          8         15  ===============
          1          0          1          0 :          8         15  ---
          1          0          2          1 :          8         15  ---
       1    2    1       1    1  1.00000000    8   15
          1          0          3          1 :          8         15  ---
       1    3    1       2    1  1.00000000    8   15
```

and annotated excerpts of its bulk part (following the two initial lines) are shown in Fig. 9.

```
 #N=     1    n0=    0       Nl=44 :         Z=8       A= 15  ===============
    #N=   1           0        l= 1       Nk= 0 :          8          15  ---
    #N=   1           0        l= 2       Nk= 1 :          8          15  ---
  #N=   1 l= 2 k= 1        1 lf=1  1.00000000    8   15
    #N=   1           0        l= 3       Nk= 1 :          8          15  ---
  #N=   1 l= 3 k= 1        2 lf=1  1.00000000    8   15
    #N=   1           0        l= 4       Nk= 1 :          8          15  ---
  #N=   1 l= 4 k= 1        3 lf=1  1.00000000    8   15
---- decays from levels l=5:43 in nuclide #1 ----
   #N=     1           0        l=44       Nk=43 :          8          15  ---
  #N=   1 l=44 k= 1      636 lf=1  0.22932881    8   15
  #N=   1 l=44 k= 2      637 lf=4  0.33386502    8   15
---- decays k=3:42 from level l=44 in nuclide #1 ----
  #N=   1 l=44 k=43      678 f=43  1.00000000    8   15
   #N=     2    n0=   44       Nl=29 :         Z=8       A= 16  ===============
    #N=   2           44        l= 1       Nk= 0 :          8          16  ---
    #N=   2           44        l= 2       Nk= 1 :          8          16  ---
  #N=   2 l= 2 k= 1      679 lf=1  1.00000000    8   16
   #N=    2     n0=  44        l= 3       Nk= 1 :          8          16  ---
  #N=   2 l= 3 k= 1      680 lf=1  1.00000000    8   16
   #N=    2    n0=   44       l=  4       Nk= 3 :          8          16  ---
  #N=   2 l= 4 k= 1      681 lf=1  0.99965018    8   16
  #N=   2 l= 4 k= 2      682 lf=2  0.99992007    8   16
  #N=   2 l= 4 k= 3      683 lf=3  1.00000000    8   16
---- decays from levels l=5:28 from nuclide #2 ----
   #N=      2    n0=   44        l=29      Nk=28 :          8          16  ---
  #N=   2 l=29 k= 1      904 lf=3  0.36608791    8   16
  #N=   2 l=29 k= 2      905 lf=4  0.54643500    8   16
---- decays k=3:28 from level l=29 in nuclide #2 ----
  #N=   2 l=29 k=27      930 f=27  0.99999970    8   16
  #N=   2 l=29 k=28      931 f=28  1.00000000    8   16
---- decays from nuclei #N=3:1195 ---
   #N=  1196    n0=35452       Nl=33 :        Z=80       A=204  ===============
    #N=1196       35452        l= 1       Nk= 0 :         80         204  ---
    #N=1196       35452        l= 2       Nk= 1 :         80         204  ---
  #N=1196 l= 2 k= 1   266873 lf=1  1.00000000   80  204
---- decays from levels l=3:32 in nuclide #1196 ----
    #N=1196       35452        l=33       Nk= 2 :         80         204  ---
  #N=1196 l=33 k= 1   266935 f=18  0.76749998   80  204
  #N=1196 l=33 k= 2   266936 f=16  1.00000000   80  204
  #N=   1197    n0=35485       Nl=9 :         Z=80       A=205  ===============
    #N=1197       35485        l= 1       Nk= 0 :         80         205  ---
    #N=1197       35485        l= 2       Nk= 1 :         80         205  ---
  #N=1197 l= 2 k= 1   266937 lf=1  1.00000000   80  205
------ decays from levels l=3:8 in nuclide #1197 ----
    #N=1197       35485        l= 9       Nk= 2 :         80         205  ---
  #N=1197 l= 9 k= 1   266949 lf=7  0.82760000   80  205
  #N=1197 l= 9 k= 2   266950 lf=6  1.00000000   80  205
```

Figure 9: Annotated excerpt of the data file `Fij.dat`.

After the descriptive headline follows a line giving the total number of decays included. Then follows the bulk of the file which is nested according to the nuclide considered, #N, its levels, $\ell = 1, n_\ell(N)$, and the decays from those levels, $k = 1, n_\gamma(N,\ell)$. (In the annotations, n_ℓ is denoted as `Nl` and n_γ as `Nk`.)

At the top level there is an introductory line giving the global index of the nuclide, #N, the cumulative number of levels (denoted by `n0`) which is zero for the first nuclide, and the number of contributing levels n_ℓ (indicated as `Nl`) for that nuclide. The values of Z and A are also given (but only for convenience - they are not being read in). At the intermediate nesting level, there is a data line for each level $\ell = 1, n_\ell$ giving n_γ (shown as `Nk`), the number of decays from that particular level. The ground state corresponds to $\ell = 1$ and has no decays, $n_\gamma(\ell = 1) = 0$. We also note that the cumulative number of levels up to the last nuclide (#N=1197) is n0=35485,

so that adding the number of levels associated with the last nuclide, $n_\ell(1197) = 9$, indeed yields the previously stated total number of levels, 35494.

Finally, at the innermost level, there is one line for each of the n_γ decays specifying the final level ℓ_f (denoted as `lf` or simply `f` where space is tight) and the associated cumulative probability $F_{ij}(k)$,

$$F_{ij}(k) \;=\; \sum_{k'=1}^{k} P(\ell \to \ell_f(k')) \;,$$

where $P(\ell_i \to \ell_f)$ denotes the branching ratio for the decay from the level ℓ_i to the level ℓ_f. We note that $F_{ij}(k)$ increases monotonically from the first (and largest) branching ratio $P(\ell \to \ell_f(k=1))$ to unity as k is increased from one to n_γ. The sampling of the decay branch k can therefore be made by generating a random number $\eta \in [0,1)$ and determining the lowet value of k for which $F_{ij}(k)$ exceeds η.

Table 22: Description of structure for top level of data file 'Fij.dat'

column	description
1	Index of isotope (Z,A), runs from 1 to 1197
2	Last level of previous nucleus
3	Number of levels for given (Z,A)
4	Proton number Z
5	Mass number A
6	'====' Separator

Note that for column 2 in the top level, for the first nucleus, the last level of the previous nucleus does not exist so it is given the value of zero for $(Z,A) = (8,15)$.

Table 23: Description of structure for second level of data file 'Fij.dat'

column	description
1	Index of isotope (Z,A), runs from 1 to 1197
2	Last level of previous nucleus
3	Index of level for particular (Z,A)
4	Number of decays from that level
5	Proton number Z
6	Mass number A
7	'—' Separator

In the two upper levels of the data file Fij.dat, there is a ":" placed as a separator between the level information and the Z and A of the isotope. There are also different separators "======" in the top level and "—" in the second level to help guide the eye of anyone perusing the data file. They are not used but help make it more human readable.

The levels are arranged so that the lowest decay probability for a given level is first, highest last. This is not necessarily in the same order as in the original table. The data have been sorted for fastest searching. The decay probabiliies are renormalized so that the probability for the last decay in the list is exactly unity.

Table 24: Description of structure for third level of data file 'Fij.dat'

column	description
1	Index of isotope (Z,A), runs from 1 to 1197
2	Index of level for particular (Z,A)
3	Index of decay for given level of (Z,A)
4	Index of decay, cumulative, goes from 1 to 266950
5	Daughter level index for particular decay
6	Decay probability of this level
7	Proton number Z
8	Mass number A

The index for the daughter level in column 5 of the third level of file Fij.dat is not sequential and may seem incomplete. This index is taken from the RIPL-3 table. Note that in FREYA, only the probabilities for photon emission have been retained. The probabilities for decay by electromagnetic transitions are not kept because FREYA does not include these transitions. The coefficients for internal conversion are also not retained in Fij.dat.

4 Running FREYA

This section illustrates how to use FREYA within the LLNL Fission Library. Some short codes are presented, both employing application programmable interfaces (APIs). The first uses the C++ API, while the second uses the C API. They both create a histogram exhibiting the angular correlation between two neutrons emitted during fission.

4.1 Integration of FREYA in LLNL Fission Library

FREYA was first integrated into the LLNL Fission Library, which already provided an existing interface to MCNPX and MCNP6. Conveniently, no modification of MCNPX/MCNP6 was necessary after the LLNL Fission Library was substituted in the source code tree.

Currently, FREYA selects outgoing projectiles from spontaneous and neutron-induced fission for incident neutron energies below 20 MeV. Photofission is planned for the near future. For each spontaneous or neutron-induced fission event, the code checks whether the sampled isotope is available in FREYA. If present, FREYA is called to sample multiplicity, energy, and direction of the fission neutrons, all of which are passed back to the LLNL Fission Library and eventually to MCNP for transport. All other fission events are handled by the default LLNL Fission Library settings in the usual way. When in use, FREYA predicts a host of correlations between outgoing fission products: correlations in neutron multiplicity, energy and angles, and energy sharing between neutrons and photons.

4.2 Verification

We verified [37] that FREYA is yielding the correct average neutron induced fission spectrum within MCNP by calculating the criticality parameter k_{eff} for the critical assemblies Godiva and Jezebel [38]. The k_{eff} results using FREYA were 0.9994 ± 0.0009 (Jezebel) and 1.0003 ± 0.0008 (Godiva), in good agreement with the default MCNP values.

4.3 Setting up the environment

The LLNL Fission Library/FREYA package is available at the following URL: http://nuclear.llnl.gov/simulation/. The FREYA part of the package is written in Fortran 90 and has been tested with both gfortran and the Intel Fortran compiler. A standard Makefile builds the LLNL Fission Library/FREYA as a static library, which can then be linked in with host radiation transport codes.

In order to run, the environment variable **FREYADATAPATH** must point to the directory containing the data files used by FREYA. In the bash shell, this can be done with the following statement:

export FREYADATAPATH=/path/to/freya/data/directory/ .

If unspecified, the LLNL Fission Library will look into the directory "./data" to find the data for FREYA.

4.4 Error conditions and limitations

If a valid location for the data is not found, an error message will be generated and the LLNL Fission Library will run under correlation option 0 (see Sec. A.1.7), that is without FREYA turned on.

If a reaction (spontaneous fission or neutron-induced fission) for an isotope is not specified in the master data file "react.data", an error message will be generated and the LLNL Fission Library will temporarily revert to correlation option 0 (see Sec. A.1.7) for this reaction. The same happens if the energy of an incident neutron is greater than 20 MeV or if one of the error conditions described in Sec. 3 occurs.

Error messages can be retrieved by the user, see Secs. A.1 and A.2.

4.5 Code using C++ API

This first code uses the C++ interface described in Sec. A.1 to invoke the LLNL Fission Library:

```
#define iterations 3000000
#define nbins 100

#include <stdio.h>
#include "fissionEvent.h"

void init(void);
FILE* openfile(char* name);
void output(int* hist);

int main() {
   int isotope = 94239;
   double energy_MeV = 2.;
   double nubar = 3.163;
   double time = 0.;

   int maxerrorlength=10000;
   char errors[maxerrorlength];

   int hist[nbins];
   for (int i=0; i<nbins; i++) hist[i] = 0.;

   init();
   for (int i=0; i<iterations; i++) {
      fissionEvent* fe = new fissionEvent(isotope, time, nubar, energy_MeV, 1);
      int errorlength=maxerrorlength;
      fe->getFREYAerrors(&errorlength, &errors[0]);
      if (errorlength>1) {
```

```
         printf("%s\n",errors);
         exit(1);
      }
      int nneutrons = fe->getNeutronNu();
      for(int n1=0; n1<nneutrons; n1++) {
         double u1 = fe->getNeutronDircosu(n1), v1 = fe->getNeutronDircosv(n1), w1 = fe->getNeutronDircosw(n1);
         for(int n2=n1+1; n2<nneutrons; n2++) {
            double u2 = fe->getNeutronDircosu(n2), v2 = fe->getNeutronDircosv(n2), w2 = fe->getNeutronDircosw(n2);
            double scalar_product = u1*u2+v1*v2+w1*w2;

            int bin_index = (int) (nbins*(scalar_product+1)/2);
            hist[bin_index]++;
         }
      }
      delete fe;
   }
   output(hist);
}

void init(void) {
   unsigned short int s[3] = {1234, 5678, 9012};
   int i;
   seed48(s);
   fissionEvent::setCorrelationOption(3);
   return;
}

FILE* openfile(char* name) {
   FILE* fp = fopen(name, "w");
   if (fp == (FILE *) 0) fprintf(stderr, "Could not open %s for writing", name);
   return fp;
}

void output(int* hist) {
   char filename [1024];
   sprintf(filename, "freya_correlations.res");
   FILE* fp = openfile(filename);

   unsigned int sum=0;
   for (int i=0; i<nbins; i++) sum += hist[i];
   for (int i=0; i<nbins; i++) fprintf(fp, "%e - %e : %e\n", -1+2.*i/nbins, -1+2.*(i+1)/nbins, 1.*hist[i]/sum);

   fclose(fp);
   return;
}
```

In the initialization phase, the random number generator is seeded, the call to **fissionEvent::setCorrelationOption(3)** turns on FREYA. A new instance of class fissionEvent is created for each new fission, from which we extract the directions of the emitted neutrons. Potential error messages produced by FREYA can be retrieved by the programmer via a call to **fissionEvent::getFREYAerrors()**. An example of such error is failure to specify a valid location for FREYA's data using **FREYADATAPATH**.

This code produces an output file with the distribution of angles between fission neutrons. This distribution is shown in Fig. 10.

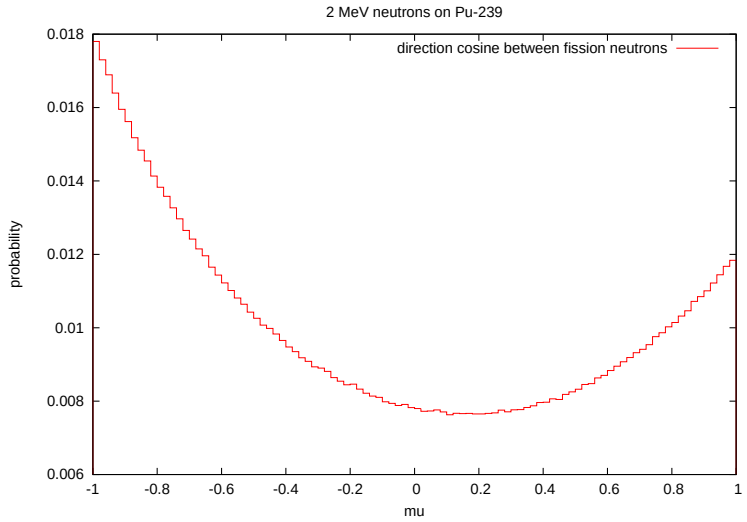

Figure 10: Distribution of angles between neutrons emitted by fission of ^{239}Pu induced by 2 MeV neutrons.

4.6 Code using C API

The same code can interface with the LLNL Fission Library using the C interface described in Sec. A.2:

```
#include "Fission.h"

int main() {
   int isotope = 94239;
   double energy_MeV = 2.;
   double nubar = 3.163;
   double time = 0.;

   int i, hist[nbins];
   for (i=0; i<nbins; i++) hist[i] = 0.;

   init();
   for (i=0; i<iterations; i++) {
      genfissevt_(&isotope, &time, &nubar, &energy_MeV);
      int nneutrons = getnnu_();
      int n1;
      for(n1=0; n1<nneutrons; n1++) {
         double u1 = getndircosu_(&n1), v1 = getndircosv_(&n1), w1 = getndircosw_(&n1);
         int n2;
         for(n2=n1+1; n2<nneutrons; n2++) {
            double u2 = getndircosu_(&n2), v2 = getndircosv_(&n2), w2 = getndircosw_(&n2);
            double scalar_product = u1*u2+v1*v2+w1*w2;

            int bin_index = (int) (nbins*(scalar_product+1)/2);
            hist[bin_index]++;
         }
      }
   }
```

```
   output(hist);

   int errorlength=10000;
   char errors[errorlength];
   getfreya_errors_(&errorlength, &errors[0]);
   if (errorlength>1) printf("%s\n",errors);
}

void init(void) {
   unsigned short int s[3] = {1234, 5678, 9012};
   int i, three = 3;
   seed48(s);
   setcorrel_(&three);
   return;
}
```

Some sections from this code were removed because they are identical to those presented in Sec. 4.5.

5 Conclusion

This manual describes the event-by-event fission generator FREYA and its integration into the LLNL Fission Library. The upgraded LLNL Fission Library was used within MCNPX2.7.0 to run Monte Carlo neutron transport simulations and to verify that results conformed to expectations for criticality benchmarks.

This new FREYA capability enables the simulation of correlations that are not predicted by conventional neutron Monte Carlo codes. For instance, angular correlations of fission neutrons that have been measured in the past could be verified using FREYA [39].

Several improvements of FREYA are planned, such as the addition of more isotopes, and photofission. We are working with the stochastic neutron transport community to make the LLNL Fission Library/FREYA package publicly available to the wider community.

6 Acknowledgments

This work performed under the auspices of the U.S. Department of Energy by Lawrence Livermore National Laboratory under Contract DE-AC52-07NA27344 and by Lawrence Berkeley National Laboratory under Contract DE-AC02-05CH11231. The authors wish to acknowledge the Office of Defense Nuclear Nonproliferation Research and Development in DOE/NNSA for their support.

A Application programmable interfaces (APIs)

FREYA is accessed via the API to the LLNL Fission Library. There are currently two different APIs in C and in C++. A description of the full interface can be found in Ref. [12]. The parts of the APIs that are relevant to FREYA will be presented here.

A.1 C++ API

The C++ interface to the LLNL fission library consists of a number of C++ functions, the functions that are relevant to FREYA will be described below:

A.1.1 fissionEvent(int isotope, double time, double nubar, double eng, int fissiontype, double* ndir=NULL)

The constructor of class **fissionEvent**. It is called to generate a fission event. Multiple neutrons and photons are generated and stored in a stack along with their energies, directions and emission times. The arguments of this function are:

isotope:	entered in the form *ZA* (e.g. 94239 for ^{239}Pu).
time:	time of the spontaneous fission.
nubar:	user-specified average number of neutrons emitted per fission (e.g. as tabulated in the cross section libraries used by the particle transport code).
eng:	energy of the neutron that induces fission.
fissiontype:	type of fission: 0) spontaneous fission, 1) neutron-induced fission, 2) photofission.
ndir:	normalized incident neutron direction, array with three elements (u,v,w).

Either the average number $\overline{\nu}$ of neutrons emitted per fission or the energy **eng** of the fission inducing neutron will be used to determine the number of neutrons sampled, see the function **setNudistOption()** below. The number of photons sampled only depends on $\overline{\nu}$. When FREYA is in use, neither $\overline{\nu}$ or **eng** is used.

The direction **ndir** of the incident neutron is only used by the FREYA model. When **ndir** is set to NULL, FREYA samples the incident neutron direction randomly.

A.1.2 ~fissionEvent()

Destructor.

A.1.3 int getNeutronNu()
int getPhotonNu()

These functions return the numbers of fission neutrons and photons emitted in the fission reaction, or -1 if no number could be sampled in the fission library due to lack of data. The reader is referred to the physics reference manual to find the list of isotopes for which sampling will return positive numbers.

A.1.4 double getNeutronEnergy(int index), double getPhotonEnergy(int index)
double getNeutronVelocity(int index), double getPhotonVelocity(int index)

These functions return the energies and velocities of the neutrons and photons.

A.1.5 double getNeutronDircosu(int index), double getNeutronDircosv(int index), double getNeutronDircosw(int index) double getPhotonDircosu(int index), double getPhotonDircosv(int index), double getPhotonDircosw(int index)

These two function families return the direction cosines of the fission neutron and photon velocity vectors along the x, y and z axes.

A.1.6 double getNeutronAge(int index) double getPhotonAge(int index)

These functions returns the age of the fission neutrons and photons, or -1 if index is out of range. Currently, delayed fission neutrons and photons are not implemented. Thus all fission products are the result of prompt emission.

A.1.7 static void setCorrelationOption(int correlation)

This function is called to set the type of neutron-photon correlation. The argument **correlation** is set to

0 (default)	for no correlation between neutrons and photons.
1	if the total fission neutron energy and total fission photon energy are sampled from normal distributions with means given in Beck *et al.* [40]. There is no correlation between the number of neutrons and the number of photons.
2	if the total fission neutron energy and total fission photon energy are sampled from normal distributions with means given in Vogt [41]. There is no correlation between the number of neutrons and the number of photons.
3	for the FREYA mode. The neutrons and photons are correlated in number and energy. If isotope can not be handled by `FREYA`, **correlation** reverts back to correlation option 0.

When **correlation** is set to 3 and `FREYA` can handle the isotope, **setNudistOption()** and **setCf252Option()** settings are bypassed. `FREYA` computes all secondary observables independently.

A.1.8 static void setNudistOption(int nudist)

This selects the data to be sampled for the neutron number distributions in the case of neutron-induced fission. If there are no data available, then the Terrell approximation is used for all cases. The argument **nudist** takes 4 values.

0	Use the fit to the Zucker and Holden tabulated $P(\nu)$ distributions as a function of energy for ^{235}U, ^{238}U and ^{239}Pu [42].
1	Use fits to the Zucker and Holden tabulated $P(\nu)$ distribution as a function of energy for ^{238}U and ^{239}Pu [42], and a fit to the Zucker and Holden data [42] as well as the Gwin, Spencer and Ingle data (at thermal energies) [43] as a function of energy for ^{235}U.
2	Use the fit to the Zucker and Holden tabulated $P(\nu)$ distributions as a function of $\overline{\nu}$ [42]. The ^{238}U fit is used for the ^{232}U, ^{234}U, ^{236}U and ^{238}U isotopes, the ^{235}U fit for ^{233}U and ^{235}U, the ^{239}Pu fit for ^{239}Pu and ^{241}Pu.
3 (default)	Use the discrete Zucker and Holden tabulated $P(\nu)$ distributions and corresponding values of $\overline{\nu}$ [42]. Sampling based on the incident neutron $\overline{\nu}$. The ^{238}U data tables are used for the ^{232}U, ^{234}U, ^{236}U and ^{238}U isotopes, the ^{235}U data for ^{233}U and ^{235}U, the ^{239}Pu data for ^{239}Pu and ^{241}Pu.

A.1.9 static void setCm244Option(int ndist)

This function is specific to the spontaneous fission of ^{244}Cm. It was introduced in version 2.0.2 of the `LLNL Fission Library`. It selects the data to be sampled for the neutron number distribution and takes the following argument:

ndist: Sample the number of neutrons
- 0 (default) from the tabulated data measured by Holden and Zucker [44]
- 1 from Vorobyev's data [45]

A.1.10 static void setCf252Option(int ndist, int neng)

This function is specific to the spontaneous fission of ^{252}Cf. It selects the data[4] to be sampled for the neutron number and energy distributions and takes the following arguments:

ndist: Sample the number of neutrons
- 0 (default) from the tabulated data measured by Spencer [46].
- 1 from the Boldeman data [47].
- 2 from Vorobyev's data [45]

neng: Sample the spontaneous fission neutron energy
- 0 (default) from the Mannhart-corrected Maxwellian spectrum [48].
- 1 from the Madland-Nix model spectrum [32].
- 2 from the Watt spectrum [49] fit attributed to Fröhner [50].

A.1.11 static void setRNGf(float (*funcptr) (void)), static void setRNGd(double (*funcptr) (void))

This function sets the random number generator to the user-defined one specified in the argument. If either **setRNGf()** or **setRNGd()** are not specified, the default system call **srand48** is used. The arguments are random number generator functions that returns variables of type float and double respectively. The C++ language imposes that the function pointer in argument be either a global function or a static function of another class.

A.1.12 void getFREYAerrors(int* length, char* errors)

This function returns potential error messages generated by FREYA. The arguments of this function are

length: length of array of characters.
errors: pointer to an allocated array of characters.

A.1.13 void setFREYAdatapath(char* datapath)

This function is called to set the path to the directory where the data required by `FREYA` is located. It takes the following argument:

path: pointer to a character string containing the path to the directory containing the data required by `FREYA`.

[4] The Vorobyev data was introduced in version 2.0.2 of the `LLNL Fission Library`.

A.2 C API

The C interface to the LLNL fission library consists of 29 C functions, the functions that are relevant to FREYA will be described below:

A.2.1 void genspfissevt_(int *isotope, double *time)

This function is called to trigger a spontaneous fission event. Multiple neutrons and photons are generated and stored in a stack along with their energies, directions and emission times. The arguments of this function are

isotope: entered in the form *ZA* (e.g. 94239 for ^{239}Pu)
time: time of the spontaneous fission event.

The generated neutrons and photons, along with their properties, will be lost upon the next call to **genspfissevt_()** or **genfissevt_()**. Therefore, they must be retrieved by the caller before a subsequent call to one of these functions, using the appropriate functions described below.

A.2.2 void genfissevtdir_(int *isotope, double *time, double *nubar, double *eng, double *ndir)

This function is called to trigger a neutron-induced fission event. In addition to the two arguments above for **genspfissevt_()**, the fission-inducing neutron is characterized by:

nubar: user-specified average number of neutrons emitted per fission (e.g. as tabulated in the cross section libraries used by the particle transport code)
eng: energy of the neutron that induces fission.
ndir: normalized incident neutron direction, array with three elements (u,v,w).

Either the average number $\overline{\nu}$ of neutrons emitted per fission or the energy **eng** of the fission inducing neutron will be used to determine the number of neutrons sampled, see the function **setnudist_()** below. The number of photons sampled only depends on $\overline{\nu}$. Similar to **genspfissevt_()**, the generated neutrons and photons are lost upon subsequent calls to **genspfissevt_()** or **genfissevt_()**.

The direction **ndir** of the incident neutron is only used by the `FREYA` model.

A.2.3 void genfissevt_(int *isotope, double *time, double *nubar, double *eng)

Same as call to **genfissevtdir_()** but `FREYA` samples the incident neutron direction randomly.

A.2.4 int getnnu_()
int getpnu_()

These functions are the counterparts of those in Sec. A.1.3.

A.2.5 double getneng_(int *index), double getpeng_(int *index)
double getnvel_(int *index), double getpvel_(int *index)

These functions are described in Sec. A.1.4.

A.2.6 double getneng_(int *index), double getpeng_(int *index) double getnvel_(int *index), double getpvel_(int *index)

These functions are identical to those in Sec. A.1.4.

A.2.7 double getndircosu_(int *index), double getndircosv_(int *index), double getndircosw_(int *index) double getpdircosu_(int *index), double getpdircosv_(int *index), double getpdircosw_(int *index)

These functions are explained in Sec. A.1.5.

A.2.8 double getnage_(int *index) double getpage_(int *index)

These functions are the counterparts of those in Sec. A.1.6.

A.2.9 void setcorrel_(int *correlation)

This function is explained in Sec. A.1.7.

A.2.10 void setnudist_(int *nudist)

This function has its counterpart in Sec. A.1.8.

A.2.11 void setcm244_(int *ndist, int *neng)

This function is described in Sec. A.1.9.

A.2.12 void setcf252_(int *ndist, int *neng)

This function is described in Sec. A.1.10.

A.2.13 void setrngf_(float (*funcptr) (void)), void setrngd_(double (*funcptr) (void))

These functions have their counterpart in Sec. A.1.11.

A.2.14 void getfreya_errors(int* length, char* errors)

This function has a counterpart in Sec. A.1.12.

A.2.15 void setfreyadatapath(char* datapath)

The counterpart of this function is described in Sec. A.1.13.

References

[1] X-5 Monte Carlo Team, "MCNP – A General Monte Carlo N-Particle Transport Code, Version 5 - Volume I: Overview and Theory," Los Alamos National Laboratory, Los Alamos, NM, LA-UR-03-1987 (2008). 4

[2] X-5 Monte Carlo Team, "MCNP – A General Monte Carlo N-Particle Transport Code, Version 5 - Volume II: User's Guide," Los Alamos National Laboratory, Los Alamos, NM, LA-CP-03-0245 (2003). 4

[3] X-5 Monte Carlo Team, "MCNP – A General Monte Carlo N-Particle Transport Code, Version 5 - Volume III: Developer's Guide," Los Alamos National Laboratory, Los Alamos, NM, LA-CP-03-0284 (2003). 4

[4] T. Goorley et al. "Initial MCNP6 Release Overview - MCNP6 version 1.0," Los Alamos National Laboratory, Los Alamos, NM, LA-UR-13-22934 (2013). 4

[5] Available from the Radiation Safety Information Computational Center, http://rsicc.ornl.gov. 4

[6] D. E. Cullen, "TART2005: A Coupled Neutron-Photon 3-D, Combinatorial Geometry, Time Dependent Monte Carlo Transport Code," Lawrence Livermore National Laboratory, Livermore CA, UCRL-SM-218009 (2005). 4

[7] R. M. Buck and E. M. Lent, "COG User's Manual: A Multiparticle Monte Carlo Transport Code," Lawrence Livermore National Laboratory, Livermore CA, UCRL-TM-202590, 5th Edition (2002). 4

[8] Available from the European Organization for Nuclear Research, http://geant4.cern.ch. 4

[9] T. E. Valentine, "MCNP-DSP Users Manual," Oak Ridge National Laboratory, Oak Ridge, TN, ORNL/TM-13334 R2 (January 2001). 4

[10] E. Padovani, S. A. Pozzi, S. D. Clarke and E. C. Miller, "MCNPX-PoliMi User's Manual," C00791 MNYCP, Radiation Safety Information Computational Center, Oak Ridge National Laboratory (2012). 4

[11] D. B. Pelowitz et al., "MCNPX2.7.0 Extensions," Los Alamos National Laboratory, Los Alamos, NM, LA-UR-11-02295 (2011). 4

[12] J. M. Verbeke, C. Hagmann and D. Wright, "Simulation of Neutron and Gamma-Ray Emission from Fission and Photofission," Lawrence Livermore National Laboratory, Livermore CA, UCRL-AR-228518 (2010). 4, 39

[13] S. Lemaire, P. Talou, T. Kawano, M. B. Chadwick and D. G. Madland, "Monte Carlo approach to sequential neutron emission from fission fragments," Phys. Rev. C **72**, pp. 024601-1-12 (2005). 4, 11

[14] S. Lemaire, P. Talou, T. Kawano, M. B. Chadwick and D. G. Madland, "Monte Carlo approach to sequential γ-ray emission from fission fragments," Phys. Rev. C **73**, pp. 014602-1-9 (2006). 4

[15] J. Randrup and R. Vogt, "Calculation of fission observables through event-by-event simulation," Phys. Rev. C **80**, pp. 024601-1-11 (2009). 4, 8

[16] R. Vogt, J. Randrup, J. Pruet and W. Younes, "Event-by-event study of prompt neutrons from ^{239}Pu(n,f)," Phys. Rev. C **80**, pp. 044611-1-16 (2009). 4

[17] R. Vogt and J. Randrup, "Event-by-event study of neutron observables in spontaneous and thermal fission," Phys. Rev. C **84**, pp. 044621-1-14 (2011). 4, 8, 11

[18] R. Vogt, J. Randrup, D. A. Brown, M. A. Descalle and W. E. Ormand, "Event-by-event evaluation of the prompt fission neutron spectrum from ^{239}Pu(n,f)," Phys. Rev. C **85**, pp. 024608-1-18 (2012). 4, 5, 6, 7, 8, 9, 11, 12, 22, 27

[19] R. Vogt and J. Randrup, "Event-by-event study of photon observables in spontaneous and thermal fission," Phys. Rev. C **87**, pp. 044602-1-16 (2013). 4, 11, 14

[20] J. Randrup and R. Vogt, "Refined treatment of angular momentum in the event-by-event fission model `FREYA`," Phys. Rev. C **89**, pp. 044601-1-6 (2014). 4, 9, 11

[21] TRIPOLI-4® Project Team: "TRIPOLI-4 version 8 User Guide," CEA-R-6316, Feb. 2013. 4

[22] J. M. Verbeke, J. Randrup and R. Vogt, "Fission Reaction Event Yield Algorithm `FREYA 2.0.2`," Lawrence Livermore National Laboratory, LLNL-JRNL-728890 (2017). 4

[23] W. J. Swiatecki, K. Siwek-Wilczyńska and J. Wilczyński, "Ratios of disintegration rates for distinct decay modes of an excited nucleus," Phys. Rev. C, **78**, pp. 054604-1-10 (2008). 6, 17

[24] W. Younes et al, "Transition from asymmetric to symmetric fission in the ^{235}U(n,f) reaction," Phys. Rev. C, **64**, pp. 054613-1-22 (2001). 8

[25] W. Reisdorf, J. P. Unik, H. C. Griffin and L. E. Glendenin, "Fission fragment K x-ray emission and nuclear charge distribution for thermal neutron fission of ^{233}U, ^{235}U, ^{239}Pu and spontaneous fission of ^{252}Cf," Nucl. Phys. A, **177**, pp. 337-378 (1971). 8

[26] G. Audi and A. H. Wapstra, "The 1995 update to the atomic mass evaluation," Nucl. Phys. A **595**, pp. 409-480 (1995). 9, 25

[27] P. Möller, J. R. Nix, W. D. Myers and W. J. Swiatecki, "Nuclear Ground-State Masses and Deformations," Atomic Data and Nucl. Data Tab. **59**, issue 2, pp. 185-381 (1995). 9, 24, 26

[28] T. Kawano, private communication. 11

[29] H. Koura, M. Uno, T. Tachibana and M. Yamada, "Nuclear mass formula with shell energies calculated by a new method," Nucl. Phys. A **674**, pp. 47-76 (2000). 11, 26

[30] V. F. Weisskopf, Phys. Rev. **52**, 295 (1937). 11

[31] J. Terrell, Phys. Rev. **113**, 527 (1959). 11

[32] D. G. Madland and J. R. Nix, "New Calculation of Prompt Fission Neutron Spectra and Average Prompt Neutron Multiplicities", Nucl. Sci. Eng. **81**, pp. 213–271 (1982). 11, 41

[33] R. Vogt and J. Randrup, "Neutron angular correlations in spontaneous and neutron-induced fission," Phys. Rev. C **90**, pp. 064623-1-7 (2014). 12

[34] R. Capote *et al.*, "RIPL – Reference Input Parameter Library for Calculation of Nuclear Reactions and Nuclear Data Evaluations," Nucl. Data Sheets **110**, pp. 3107-3214 (2009). 13, 14, 27

[35] J. Randrup and R. Vogt, in progress. 13, 14

[36] B. L. Berman and S. C. Fultz, "Measurements of the giant dipole resonance with monoenergetic photons," Rev. Mod. Phys. **47**, pp. 713-760 (1975). 14

[37] C. Hagmann, J. Randrup and R. Vogt, "FREYA A new Monte Carlo code for improved modeling of fission chains," Trans. Nucl. Sci. **60**, pp. 545-549 (2013). 34

[38] International Handbook of Evaluated Criticality Safety Benchmark Experiments, NEA Nuclear Science Committee (2007), http://icbep.inel.gov. 34

[39] J. M. Verbeke, C. A. Hagmann, J. Randrup and R. Vogt, "Integration of FREYA into MCNP6: An Improved Fission Chain Modeling Capability," Lawrence Livermore National Laboratory, LLNL-PROC-638986 (2013). 38

[40] B. Beck, D. A. Brown, F. Daffin, J. Hedstrom and R. Vogt, "Implementation of Energy-Dependent Q Values for Fission," UCRL-TR-234617, Lawrence Livermore National Laboratory (2007). 40

[41] R. Vogt, "Energy-Dependent Fission Q Values Generalized for All Actinides," LLNL-TR-407620, Lawrence Livermore National Laboratory (2008). 40

[42] M. S. Zucker and N. E. Holden, "Energy Dependence of Neutron Multiplicity $P(\nu)$ in Fast-Neutron-Induced Fission for ^{235,238}U and ^{239}Pu," BNL-38491 (1986). 40

[43] R. Gwin, R. R. Spencer and R. W. Ingle, "Measurements of the Energy Dependence of Prompt Neutron Emission from ^{233}U, ^{235}U, ^{239}Pu, and ^{241}Pu for $E_n = 0.005$ to 10 eV Relative to Emission from Spontaneous Fission of ^{252}Cf," Nucl. Sci. Eng. **87**, pp. 381–404 (1984). 40

[44] N.E. Holden, M.S. Zucker, "A Reevaluation of the Average Prompt Neutron Emission Multiplicity ($\bar{\nu}$) Values from Fission of Uranium and Transuranium Nuclides," BNL-NCS-35513, Brookhaven National Laboratory). 41

[45] A.S. Vorobyev, V. N. Dushin, F.-J. Hambsch, V.A. Jakovlev, V.A. Kalinin, A.B. Laptev, B.F. Petrov, O.A. Shcherbakov, "Distribution of Prompt Neutron Emission Probability for Fission Fragments in Spontaneous Fission of ^{252}Cf and ^{244,248}Cm," *AIP Conf. Proc.*, **769**, 613; doi: 10.1063/1.1945084 (2005). 41

[46] R. R. Spencer, R. Gwin and R. W. Ingle, "A measurement of the Average Number of Prompt Neutrons from Spontaneous Fission of Californium-252," Nucl. Sci. Eng. **80**, pp. 603–629 (1982). 41

[47] J. W. Boldeman and M. G. Hines, "Prompt Neutron Emission Probabilities Following Spontaneous and Thermal Neutron Fission," Nucl. Sci. Eng. **91**, pp. 114–116 (1985). 41

[48] W. Mannhart, "Evaluation of the ^{252}Cf Fission Neutron Spectrum Between 0 MeV and 20 MeV," Proc. Advisory Group Mtg. Neutron Sources, Leningrad, USSR, 1986 (IAEA-TECDOC-410), Vienna (1987). 41

[49] B. E. Watt, "Energy Spectrum of Neutrons from Thermal Fission of ^{235}U," Phys. Rev. **87**, pp. 1037–1041 (1952). 41

[50] F. H. Fröhner, "Evaluation of ^{252}Cf Prompt Fission Neutron Data from 0 to 20 MeV by Watt Spectrum Fit," Nucl. Sci. Eng. **106**, pp. 345–352 (1990). 41